RSC Advances

PAPER

View Article Online
View Journal | View Issue

Cite this: *RSC Adv.*, 2017, **7**, 41345

Synthesis and structural analysis of aryloxo-modified trinuclear half-titanocenes, and their use as catalyst precursors for ethylene polymerisation†

Qing Yan, Ken Tsutsumi and Kotohiro Nomura *

Received 10th July 2017
Accepted 16th August 2017

DOI: 10.1039/c7ra07581b

rsc.li/rsc-advances

A series of trinuclear half-titanocenes, $[Cp'TiX_2\{(O\text{-}2,4\text{-}R_2C_6H_2)\text{-}6\text{-}CH_2\}]_3N$ [X = Cl, R = Me, Cp′ = Cp (**1**); X = Cl, R = ^{t}Bu, Cp′ = Cp (**4**), Cp* (**5**), ^{t}BuC$_5$H$_4$ (**6**), 1,2,4-Me$_3$C$_5$H$_2$ (**7**); X = Me, Cp′ = Cp*, R = Me (**8**), ^{t}Bu (**9**)] and the related bimetallic complexes, $[Cp'TiCl_2\{(O\text{-}2,4\text{-}Me_2C_6H_2)\text{-}6\text{-}CH_2\}][Cp'TiCl\{(O\text{-}2,4\text{-}Me_2C_6H_2)\text{-}6\text{-}CH_2\}_2]N$ [Cp′ = Cp* (**2**), 1,2,4-Me$_3$C$_5$H$_2$ (**3**)], have been prepared and identified. Structures of **1–5**, **7** and **9** were determined by X-ray crystallography, and all complexes fold with distorted tetrahedral geometries around titanium. These complexes (**2–9**) are stable in solution except the Cp analogue (**1**), which presents as a mixture of the trinuclear analogue (**1**) and the (proposed) binuclear analogue, CpTiCl$_3$, and $CpTi[\{(O\text{-}2,4\text{-}Me_2C_6H_2)\text{-}6\text{-}CH_2\}]_3N$ in solution; there is an equilibrium between **1** and the binuclear analogue (and CpTiCl$_3$) depending on the temperature, solvent and concentration. The Cp* analogues (**2**, **8**, **9**), exhibited high catalytic activities for ethylene polymerisation in the presence of MAO cocatalyst, affording ultrahigh molecular weight polymers with uniform molecular weight distributions in most cases. $[Cp^*TiMe_2\{(O\text{-}2,4\text{-}Me_2C_6H_2)\text{-}6\text{-}CH_2\}]_3N$ (**8**) showed the higher catalytic activities than the related mononuclear analogue, $Cp^*TiCl_2(O\text{-}2\text{-}R\text{-}4,6\text{-}Me_3C_6H_2)$ (R = Me, ^{t}Bu); the activity by **8** in the presence of Al^{i}Bu$_3$–[Ph$_3$C][B(C$_6$F$_5$)$_4$] cocatalysts was higher than that in the presence of MAO.

Introduction

Transition metal catalysed olefin polymerisation is an important key reaction in the production of polyolefins [such as HDPE (high density polyethylene), LLDPE (linear low density polyethylene), isotactic polypropylene and elastomers *etc.*] in the chemical industry, and the market capacity still increases every year. Since the discovery of Ziegler-Natta catalysts, the design of efficient molecular catalysts has been considered as a key subject in terms of the synthesis of new polymers as well as of better control of molecular weights, compositions in the copolymerisations, and the development of more efficient processes.[1–5] Nowadays, many examples such as metallocenes,[1a–d,g] linked half-metallocenes (constrained geometry type),[1e] modified half-titanocenes,[4,5] and the other transition metal complex catalysts, the so called non-metallocene type,[1f,3b,c,i–k] have been reported as so called 'single-site catalysts' which facilitate the coordination and insertion polymerisation with uniform catalytically active species.[1–7] These metal complexes are generally activated by different types of cocatalysts [such as Al alkyls, methylaluminoxane (MAO), borates *etc.*][6,7] in the polymerisation to afford cationic alkyl species, which are the proposed catalytically active species in this catalysis.

Certain bimetallic olefin polymerisation catalysts (exemplified in Chart 1) have been known to exhibit unique characteristics in catalytic activity, polymer microstructure (molecular

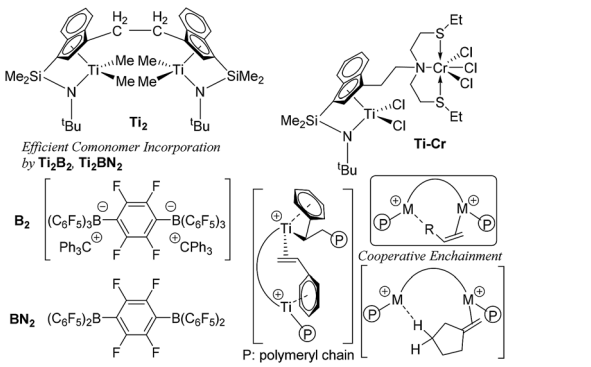

Chart 1 Typical bimetallic catalysts for efficient metal–metal cooperative effect.[3d,h,8,9]

Department of Chemistry, Tokyo Metropolitan University, 1-1 Minami Osawa, Hachioji, Tokyo 192-0397, Japan. E-mail: ktnomura@tmu.ac.jp

† Electronic supplementary information (ESI) available: (i) Additional experiments and VT ^{1}H NMR spectra of toluene-d_8 solution of $[Cp'TiCl_2\{(O\text{-}2,4\text{-}R_2C_6H_2)\text{-}6\text{-}CH_2\}]_3N$ [R = Me, Cp′ = Cp (**1**); R = ^{t}Bu, Cp′ = Cp (**4**), Cp* (**5**), ^{t}BuC$_5$H$_4$ (**6**), 1,2,4-Me$_3$C$_5$H$_2$ (**7**)], $[Cp'TiCl_2\{(O\text{-}2,4\text{-}Me_2C_6H_2)\text{-}6\text{-}CH_2\}][Cp'TiCl\{(O\text{-}2,4\text{-}Me_2C_6H_2)\text{-}6\text{-}CH_2\}_2]N$ [Cp′ = Cp* (**2**), 1,2,4-Me$_3$C$_5$H$_2$ (**3**)], additional ethylene polymerization results, and tables summarized in crystal collection parameters for **1–5** and **7–9**, and their structures reports. CCDC 1549581–1549587. For ESI and crystallographic data in CIF or other electronic format see DOI: 10.1039/c7ra07581b

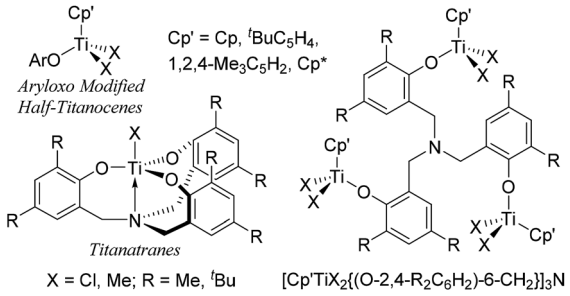

Chart 2 Reported aryloxo-modified half-titanocenes, titanatranes, and the trinuclear half-titanocenes prepared in this study.

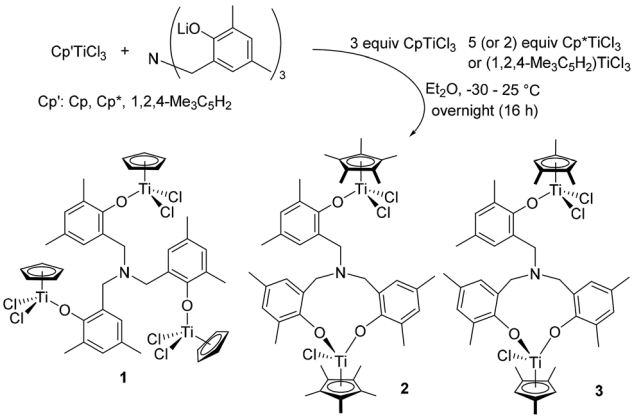

Scheme 1 Reaction of $Cp'TiCl_3$ (Cp′ = Cp, Cp*, and 1,2,4-$Me_3C_5H_2$) with $[(LiO\text{-}2,4\text{-}Me_2C_6H_2)\text{-}6\text{-}CH_2]_3N$ in Et_2O.

weight, chain branching, monomer sequences, regioregularity) compared to the monomeric analogues in olefin polymerisation[8,9] due to so called metal–metal cooperative effects.[3d,h,7a,8,9] This 'bimetallic effect' has been considered as due to their improved activation-transport (trapping/activation for subsequent comonomer incorporation on another metal center),[3d,h,8] intermolecular chain transfer and/or catalyst–cocatalyst nuclearity effect on the multi-nuclear reaction sphere,[3d,h,7a,8,9] and should be considered to provide another possibility of the new catalyst design.

Modified (nonbridged) half-titanocenes containing anionic ancillary donor ligand (Y) of type, $Cp'TiX_2(Y)$ [Cp′ = cyclopentadienyl; X = halogen, alkyl; Y = aryloxo (Chart 2), ketimide, imidazolin-2-iminato *etc.*],[4,5] have been known to display promising characteristics especially in ethylene copolymerisation with sterically encumbered olefins, styrene, cyclic olefins.[4] It has been demonstrated that both the activity and the commoner incorporation (reactivity) can be tuned by the ligand modification.[4,10] It has thus been simply assumed that design of multi-metallic half-titanocenes would facilitate activation-transport, intermolecular chain transfer on the multi-nuclear reaction sphere, which would lead to the better catalytic activity and/or better comonomer incorporation. As titanium complexes containing amine triphenolate ligands (titanatranes), $TiX[(O\text{-}2,4\text{-}R_2C_6H_2)\text{-}6\text{-}CH_2]_3N$ (Chart 2 left), displays unique catalysts for ethylene polymerisation,[11] we thus explored synthesis and structural analysis of a series of trinuclear half-titanocenes of the type, $[Cp'TiX_2\{(O\text{-}2,4\text{-}R_2C_6H_2)\text{-}6\text{-}CH_2\}]_3N$ [Chart 2 right, Cp′ = Cp, ^{t}BuC$_5$H$_4$, 1,2,4-$Me_3C_5H_2$, C_5Me_5 (Cp*); X = Cl, Me; R = Me, ^{t}Bu], and their use as the catalyst precursors for ethylene polymerisation.[12] Through this study, we wish to demonstrate some unique characteristics as the olefin polymerisation catalysts which are different from the monomeric analogues.

Results and discussion

1. Synthesis, structural analysis of trinuclear/dinuclear aryloxo-modified half-titanocenes

Trinuclear $[CpTiCl_2\{(O\text{-}2,4\text{-}Me_2C_6H_2)\text{-}6\text{-}CH_2\}]_3N$ (**1**) could be prepared by reaction of 3 equiv. of $CpTiCl_3$ with $[(LiO\text{-}2,4\text{-}Me_2C_6H_2)\text{-}6\text{-}CH_2]_3N$ in Et_2O in high yield (80%, Scheme 1). This is an analogous procedure for synthesis of aryloxo-modified half-titanocenes, $Cp'TiCl_2(OAr)$,[10i,13,14] and the complex could be identified by ^{1}H NMR spectrum, elemental analysis, and the structure was determined by X-ray crystallography (shown below, Fig. 2). In contrast, it turned out that the similar reactions with $(1,2,4\text{-}Me_3C_5H_2)TiCl_3$ and Cp^*TiCl_3, in place of $CpTiCl_3$, afforded a mixture of several complexes, and the isolated complexes were bimetallic $[Cp'TiCl_2\{(O\text{-}2,4\text{-}Me_2C_6H_2)\text{-}6\text{-}CH_2\}][Cp'TiCl\{(O\text{-}2,4\text{-}Me_2C_6H_2)\text{-}6\text{-}CH_2\}_2]N$ [Cp′ = Cp* (**2**), 1,2,4-$Me_3C_5H_2$ (**3**)] determined by X-ray crystallographic analyses (shown below, Fig. 3). Complexes **2** and **3** were also identified by NMR spectra and elemental analysis. The major products observed in ^{1}H NMR spectra were **2** or **3** (and the trichloride), even though the reaction was conducted with 5 equiv. of Cp^*TiCl_3 or $(1,2,4\text{-}Me_3C_5H_2)TiCl_3$ in Et_2O.[15] Complex **2** was also the major product observed in the ^{1}H NMR spectrum, when the reaction was conducted in toluene (shown in the ESI†).[15]

It turned out that the Cp analogue (**1**) was unstable in solution at room temperature monitored by ^{1}H NMR spectra (Fig. 1).[15] The toluene-d_8 solution containing **1** at −60 °C showed a simple NMR spectrum (marked with +) assigned as **1** (Fig. 1i, **1** 1.08×10^{-3} M), when the NMR sample (in toluene-d_8) was prepared at −30 °C (in the drybox) and kept cool until the measurement. However, the spectrum at −30 °C (Fig. 1a and j) showed resonances ascribed to **1** in addition to the others (including $CpTiCl_3$), as mentioned below. Upon increasing at −40 °C and 0 °C (Fig. 1c and d), resonance ascribed to $CpTiCl_3$ (marked with ▼) was appeared in addition to resonances ascribed to (probably) bimetallic species (marked with ○ estimated by the resonances by **2** and **3**, two doublets at 3.7–4.0 ppm and two singlets at 5.9–6.1 ppm). The intensities ascribed to $CpTiCl_3$ (and assumed bimetallic species) increased at 0 °C. The other resonances ascribed to titanatrane, $CpTi[\{(O\text{-}2,4\text{-}Me_2C_6H_2)\text{-}6\text{-}CH_2\}_3N]$[16] (marked with #) were also appeared upon increasing at 25 °C with increasing the intensities ascribed to both $CpTiCl_3$ and the assumed bimetallic species (Fig. 1e). Upon cooling, the intensity of resonances ascribed to $CpTiCl_3$ *etc.* decreased and the solution at −60 °C showed the original spectrum assigned to **1** in addition of $CpTiCl_3$ and $CpTi[\{(O\text{-}2,4\text{-}Me_2C_6H_2)\text{-}6\text{-}CH_2\}_3N]$ with ratio of *ca.* 35 : 45 : 20 (Fig. 1h), which

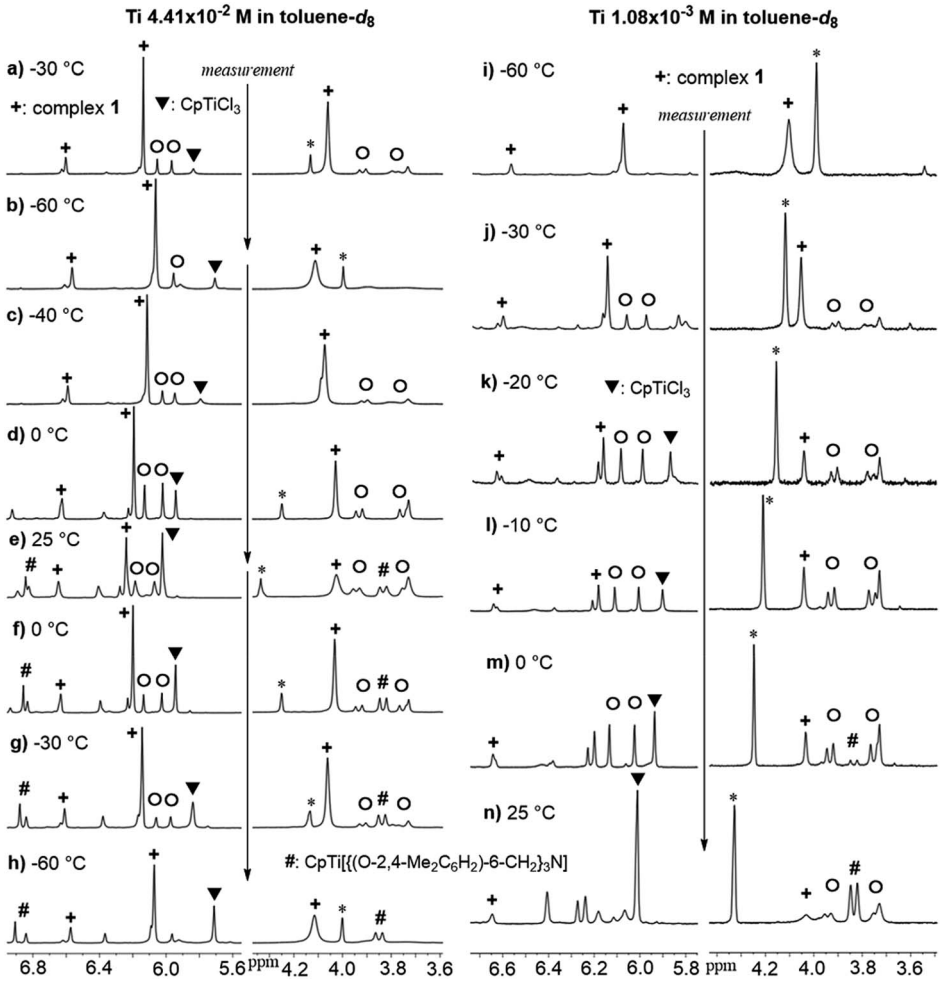

Fig. 1 Variable Temperature (VT) ^{1}H NMR spectra of toluene-d_8 solution containing [CpTiCl$_2${(O-2,4-Me$_2$C$_6$H$_2$)-6-CH$_2$}]$_3$N (**1**). Left: VT NMR spectra with rather high Ti concentration (Ti 4.41 × 10^{-2} M). Right: The VT NMR spectra with rather low Ti concentration (Ti 1.08 × 10^{-3} M). The more data are shown in the ESI.†[15] Complex **1** (+), CpTiCl$_3$ (▼), CpTi[{(O-2,4-Me$_2$C$_6$H$_2$)-6-CH$_2$}$_3$N] (#), assumed bimetallic species (○). *Impurity.

would be well suggest that the titanatrane was formed by dissociation of CpTiCl$_3$ from **1**. The similar spectra were observed when the sample of **1** was prepared with rather low concentration (Fig. 1 right), although the spectrum measured at −60 °C showed simple resonances ascribed to **1** (Fig. 1i).

Moreover, the intensity of resonances ascribed to CpTiCl$_3$ (and those in assumed bimetallic species) increased upon increasing the temperature (from −30 °C through −10 °C, Fig. 1j–l), along with decreasing the intensities of resonances ascribed to **1**.[15] Resonances ascribed to titanatrane were observed at 0 °C and the intensities increased at 25 °C. It was thus revealed from these spectra that the ratios (**1**, CpTiCl$_3$, titanatrane) were also affected by the Ti concentrations. It was also revealed that the ratio was also affected by the solvent (shown in the ESI†).[15] The integration ratios of CpTiCl$_3$ and the assumed bimetallic species were relatively close to 1 : 1, and the ratios were affected by the temperature measured and were reversible, except once formed titanatrane, CpTi[{(O-2,4-Me$_2$C$_6$H$_2$)-6-CH$_2$}$_3$N].[15,16]

These results suggest a presence of an equilibrium between **1** and the assumed bimetallic species, probably [CpTiCl$_2${(O-2,4-Me$_2$C$_6$H$_2$)-6-CH$_2$}][CpTiCl{(O-2,4-Me$_2$C$_6$H$_2$)-6-CH$_2$}$_2$]N, with dissociation of CpTiCl$_3$, as depicted in Scheme 2. The results also suggest that the further reaction could afford the titanatrane, CpTi[{(O-2,4-Me$_2$C$_6$H$_2$)-6-CH$_2$}$_3$N], with further dissociation of CpTiCl$_3$ that is very stable in solution (Scheme 2). This

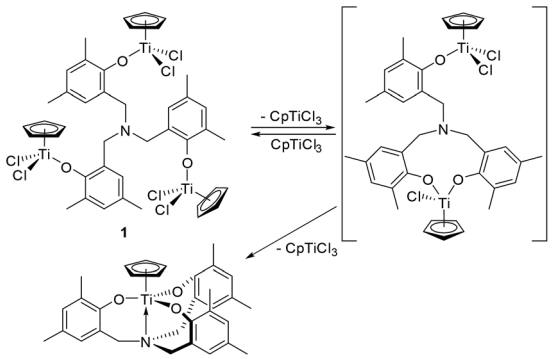

Scheme 2 Proposed equilibrium in solution containing **1** (observed in NMR spectra, Fig. 1).

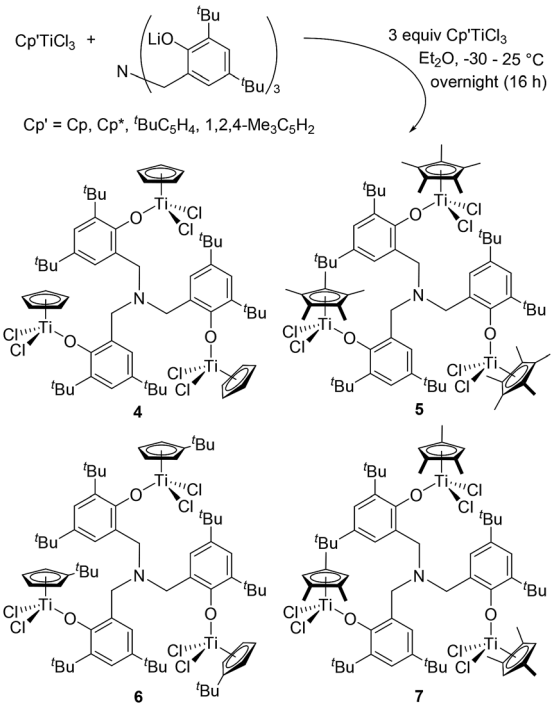

Scheme 3 Synthesis of $[Cp'TiCl_2\{(O\text{-}2,4\text{-}^tBu_2C_6H_2)\text{-}6\text{-}CH_2\}]_3N$.

assumption would be able to explain why the bimetallic **2** and **3** were isolated in the reactions of $Cp'TiCl_3$ (Cp′ = Cp*, 1,2,4-$Me_3C_5H_2$, Scheme 1). It also turned out that once formed **2** and **3** are, in contrast, relatively stable even in toluene-d_8 upon heating at 80 °C for 30 min (shown in the ESI†).[15]

It turned out that reaction of $Cp'TiCl_3$ (Cp′ = Cp, Cp*, $^tBuC_5H_4$, 1,2,4-$Me_3C_5H_2$) with $[(LiO\text{-}2,4\text{-}^tBu_2C_6H_2)\text{-}6\text{-}CH_2]_3N$ in Et_2O afforded the corresponding trinuclear complexes, $[Cp'TiCl_2\{(O\text{-}2,4\text{-}^tBu_2C_6H_2)\text{-}6\text{-}CH_2\}]_3N$ [Cp′ = Cp (**4**), Cp* (**5**), $^tBuC_5H_4$ (**6**), 1,2,4-$Me_3C_5H_2$ (**7**), Scheme 3], and the resultant complexes could be identified by NMR spectra and elemental analysis; their structures (**4**, **5**, **7**) were determined by X-ray crystallography (shown below, Fig. 2). In contrast to the methyl analogue (**1**), the *tert*-Bu complex (**4**) is relatively stable and no significant differences in the ^1H NMR spectra (in toluene-d_8) were observed upon heating at 80 °C for 30 min (shown in the ESI, Fig. S2–S6†).[15] No additional resonances were observed when the toluene-d_8 solution containing the Cp* analogue (**5**) was heated at 80 °C for 30 min (Fig. S2–S7, in the ESI†),[15] whereas certain additional resonances (but very small amount) were observed when the toluene-d_8 solutions containing the $^tBuC_5H_4$ analogue (**6**) and the 1,2,4-$Me_3C_5H_2$ analogue (**7**) were heated under the same conditions (Fig. S2–S9†).[15] The observed difference in the stability may be somewhat related to the stability and uniformity of the catalytically active species as described below.

Fig. 2 shows ORTEP drawings for the trinuclear half-titanocenes, $[CpTiCl_2\{(O\text{-}2,4\text{-}Me_2C_6H_2)\text{-}6\text{-}CH_2\}]_3N$ (**1**) and $[Cp'TiCl_2\{(O\text{-}2,4\text{-}^tBu_2C_6H_2)\text{-}6\text{-}CH_2\}]_3N$ [Cp′ = Cp (**4**), Cp* (**5**), 1,2,4-$Me_3C_5H_2$ (**7**)] determined by X-ray crystallography,[17] and the selected bond distances and the angles are summarised in

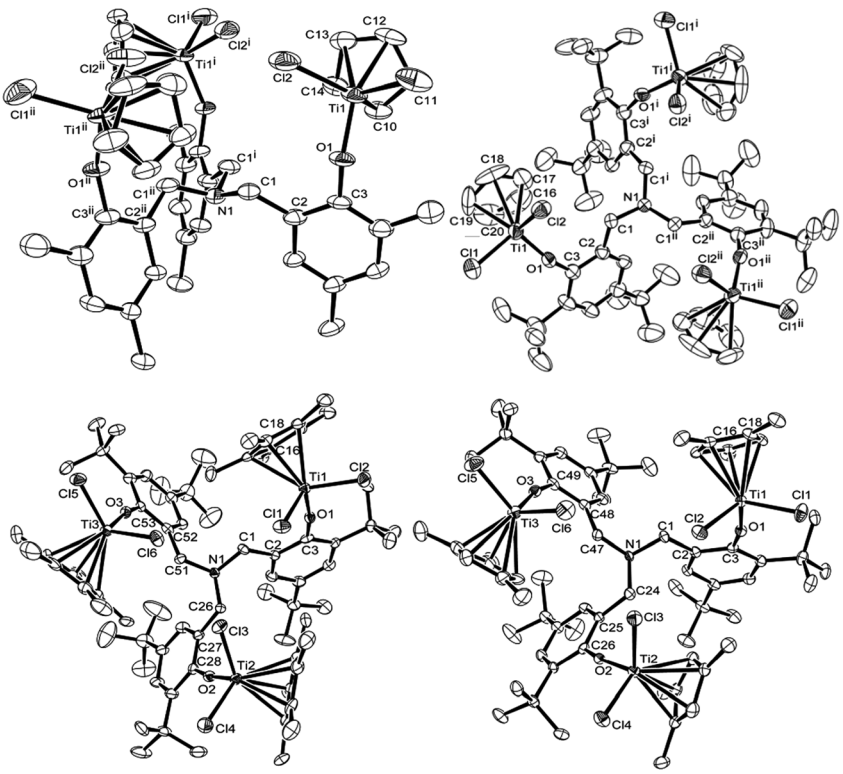

Fig. 2 ORTEP drawings for $[CpTiCl_2\{(O\text{-}2,4\text{-}Me_2C_6H_2)\text{-}6\text{-}CH_2\}]_3N$ (**1**, top left), $[Cp'TiCl_2\{(O\text{-}2,4\text{-}^tBu_2C_6H_2)\text{-}6\text{-}CH_2\}]_3N$ [Cp′ = Cp (**4**, top right), Cp* (**5**, bottom left), 1,2,4-$Me_3C_5H_2$ (**7**, bottom right)]. Thermal ellipsoids are drawn at the 50% probability level, and H atoms are omitted for clarity.[17]

Table 1 Selected bond distances and angles for $[Cp'TiCl_2\{(O\text{-}2,4\text{-}R_2C_6H_2)\text{-}6\text{-}CH_2\}]_3N$ [R = Me, Cp′ = Cp (**1**); R = ^{t}Bu, Cp′ = Cp (**4**), Cp* (**5**), 1,2,4-$Me_3C_5H_2$ (**7**)].[17]

Complex Cp′:R	**1** Cp:Me	**4** Cp:^{t}Bu	**5** Cp*:^{t}Bu	**7** 1,2,4-$Me_3C_5H_2$:^{t}Bu	$CpTiCl_2$ (O-2,6-$Et_2C_6H_3$)[a]	$CpTiCl_2$ (O-2,6-$^i Pr_2C_6H_3$)[b]	Cp*$TiCl_2$ (O-2,6-$^t Bu_2C_6H_3$)[c]
Bond distances (Å)							
Ti(1)–Cl(1)	2.252(3)	2.2649(19)	2.2616(14)	2.2615(12)	2.2680(10)	2.262(1)	2.2674(10)
Ti(1)–Cl(2)	2.249(2)	2.2361(16)	2.2702(14)	2.2475(8)	2.2710(10)	2.262(1)	2.2674(10)
Ti(1)–O(1)	1.788(4)	1.774(3)	1.790(3)	1.779(2)	1.7781(18)	1.760(4)	1.804(2)
Ti–C in Cp′	2.330(9); 2.356(9), Ti–C(10); –C(12)	2.339(8); 2.336(5), Ti–C(16); –C(18)	2.348(4); 2.415(5), Ti–C(16); –C(18)	2.343(3); 2.393(3), Ti–C(16); –C(18)	2.351(3); 2.325(3), Ti–C(1); –C(3)	2.282(8); 2.325(5), Ti–C(1); –C(3)	2.359(4); 2.370(3), Ti–C(1); –C(3)
Bond angles (°)							
Cl(1)–Ti(1)–Cl(2)	103.41(11)	101.52(6)	101.11(5)	101.14(4)	102.24(3)	104.23(7)	98.10(4)
Cl(1)–Ti–O(1)	104.50(19)	104.37(10)	103.02(10)	103.89(8)	103.35(6)	102.53(9)	103.22(6)
Cl(2)–Ti–O(1)	102.58(15)	103.17(12)	103.27(10)	104.09(8)	101.97(7)	102.53(9)	103.22(6)
Ti(1)–O–C(3)	149.9(6)	157.6(2)	169.3(3)	165.4(2)	161.37(17), Ti–O–C(11)	163.0(4), Ti–O–C(6)	155.5(2), Ti–O–C(7)
C(1)–N(1)–C(1)^i	110.6(5)	112.5(2)	110.5(3), C(1)–N(1)–C(26)	110.1(2), C(1)–N(1)–C(24)			
N(1)–C(1)–C(2)	112.8(6)	112.3(4)	111.9(3)	112.5(3)			

[a] Cited from ref. 14*d*. [b] Cited from ref. 14*c*. [c] Cited from ref. 14*f*.

Table 1. The complex **1** folds distorted tetrahedral geometry around titanium, as observed in the mononuclear half-titanocenes.[10i,14] No significant differences in the bond distances and angles were observed in each titanium complex. The Ti–Cl bond distances in **1** [2.252(3), 2.249(2) Å] are slightly shorter than those in the mononuclear analogues, $CpTiCl_2$(O-2,6-$Et_2C_6H_3$)[14d] and $CpTiCl_2$(O-2,6-$^i Pr_2C_6H_3$)[14c] [2.262(1)–2.2710(10) Å], but within the range of those in the Cp analogues containing chlorinated phenoxides like $CpTiCl_2(OC_6Cl_5)$, [2.2492(17), 2.261(3) Å].[10i] The Ti–O bond distance [1.788(4) Å] is slightly longer than those in $CpTiCl_2$(O-2,6-$Et_2C_6H_3$)[14d] and $CpTiCl_2$(O-2,6-$^i Pr_2C_6H_3$)[14c] [1.7781(18), 1.760(4) Å, respectively] but shorter than those in $CpTiCl_2(OC_6Cl_5)$ [1.814(4) Å] and $CpTiCl_2$(O-2,6-$Cl_2C_6H_3$) [1.8091(12) Å];[10i] the bond distance is, however, apparently shorter than that (1.978 Å) for Ti–O (in CF_3SO_3) bond distance in Cp*$TiMe(CF_3SO_3)$(O-2,6-$^i Pr_2C_6H_3$)[14e] due to the π-donation from oxygen to titanium. The Ti–O–C(3) (in phenyl) bond angle is 149.9(6)°, which is smaller than those in $CpTiCl_2$(O-2,6-$Et_2C_6H_3$)[14d] and $CpTiCl_2$(O-2,6-$^i Pr_2C_6H_3$)[14c] [161.37(17), 163.0(4)°, respectively] and those in the Cp analogues containing chlorinated phenoxides [151.5(3)–152.96(10)°].[10i] The Cl(1)–Ti–Cl(2) bond angle [103.41(11)°] is within the range of the reported Cp analogues [101.75(2)–104.23(7)°].[10i,14c,d]

The complexes **4**, **5** and **7** also fold a distorted tetrahedral geometry around titanium. No significant differences in the both bond distances and angles in each titanium complex were observed in the Cp analogue (**4**), whereas slight differences in both the distances and the angles were observed in the Cp* analogue (**5**) and the 1,2,4-$Me_3C_5H_2$ analogue (**7**), probably due to a steric bulk.[17] It seems likely that the Ti–Cl bond distances in the Cp* analogue [**5**, 2.2546(15)–2.2702(14) Å] is slightly longer than those in the Cp [**4**, 2.2361(16), 2.2649(19) Å] and the 1,2,4-$Me_3C_5H_2$ analogues [**7**, 2.2376(11)–2.2679(10) Å];[17] the Ti–O bond distances in **5** [1.789(3)–1.792(3) Å] are slightly longer than those in **4** [1.774(3) Å] but within the range of those in **7** [1.779(2)–1.797(2) Å]. The Ti–O–C(3) in phenyl angles increased in the order: 157.6(2)° (**4**, Cp′ = Cp) < 163.0(2)–166.7(2) (**7**, 1,2,4-$Me_3C_5H_2$) < 167.9(3)–169.8(3)° (**5**, Cp*). Moreover, the Ti–O–C bond angle in **5** is larger than that in Cp*$TiCl_2$(O-2,6-$^t Bu_2C_6H_3$) [155.5(2)°],[14c] probably due to less steric bulk. Since the observed difference in the Ti–O–C bond angle reflects the degree of O–Ti π-donation, this may explain the observed difference in the Cp* analogue (**5**) especially compared to the Cp analogue (**4**). It also seems likely that both the C(1)–N–C(1) [or C(1)–N–C(26), C(1)–N–C(24)] and N–C(1)–C(2) angles are slightly influenced by the cyclopentadienyl fragment (Table 1). As observed in the mononuclear half-titanocenes,[10i,14] it was thus revealed that these bond distances and angles are influenced by the ligand substituent.

Fig. 3 shows ORTEP drawings for the binuclear complexes, $[Cp'TiCl_2\{(O\text{-}2,4\text{-}Me_2C_6H_2)\text{-}6\text{-}CH_2\}][Cp'TiCl\{(O\text{-}2,4\text{-}Me_2C_6H_2)\text{-}6\text{-}CH_2\}_2]N$ [Cp′ = Cp* (**2**), 1,2,4-$Me_3C_5H_2$ (**3**)], determined by X-ray crystallography. These complexes fold a distorted tetrahedral geometry around each titanium metal center. In the Cp* analogue (**2**), the Ti(1)–Cl(1), Ti(1)–Cl(2), Ti(1)–O(1) bond distances [monophenoxide, 2.2830(16), 2.2787(16), 1.776(3) Å, respectively] are shorter than those in the bis(phenoxide) [Ti(2)–Cl(3), Ti(2)–O(2), Ti(2)–O(3): 2.3140(15), 1.804(3), 1.806(3) Å, respectively], whereas there were no significant differences in the Ti–O–C (in phenyl) angles were observed [Ti(1)–O(1)–C(3), Ti(2)–O(2)–C(22), Ti(2)–O(3)–C(31): 172.4(3), 173.9(3), 174.0(3)°, respectively]. Therefore, the observed difference in the bond distances would be due to degree of π-donation from oxygen to

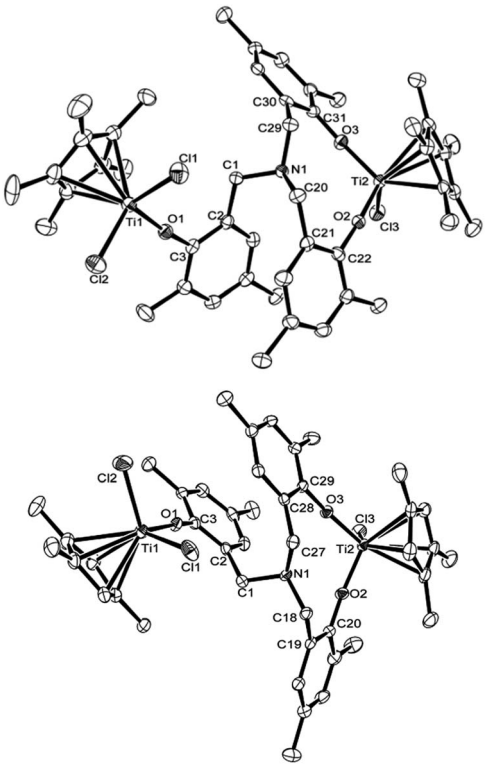

Fig. 3 ORTEP drawings for $[Cp'TiCl_2\{(O\text{-}2,4\text{-}Me_2C_6H_2)\text{-}6\text{-}CH_2\}][Cp'TiCl\{(O\text{-}2,4\text{-}Me_2C_6H_2)\text{-}6\text{-}CH_2\}_2]N$ [Cp′ = Cp* (**2**, left), 1,2,4-$Me_3C_5H_2$ (**3**, right)]. Thermal ellipsoids are drawn at the 50% probability level, and H atoms are omitted for clarity.[17] Selected bond distances (Å) and angles (°) in **2**: Ti(1)–Cl(1) 2.2830(16), Ti(1)–Cl(2) 2.2787(16), Ti(1)–O(1) 1.776(3), Ti(2)–Cl(3) 2.3140(15), Ti(2)–O(2) 1.804(3), Ti(2)–O(3) 1.806(3), N(1)–C(1) 1.461(5), N(1)–C(20) 1.471(5), N(1)–C(29) 1.474(5) Å; Cl(1)–Ti(1)–Cl(2) 103.17(5), Cl(1)–Ti(1)–O(1) 102.65(10), Cl(2)–Ti(1)–O(1) 102.46(10), Cl(3)–Ti(2)–O(2) 100.78(10), Cl(3)–Ti(2)–O(3) 100.50(11), O(2)–Ti(2)–O(3) 108.14(12), Ti(1)–O(1)–C(3) 172.4(3), Ti(2)–O(2)–C(22) 173.9(3), Ti(2)–O(3)–C(31) 174.0(3), C(1)–N(1)–C(20) 112.2(3), C(1)–N(1)–C(29) 110.3(3), C(20)–N(1)–C(29) 110.0(3), N(1)–C(1)–C(2) 113.5(3), N(1)–C(20)–C(21) 113.8(3), N(1)–C(29)–C(30) 112.9(3)°. Selected bond distances (Å) and angles (°) in **3**: Ti(1)–Cl(1) 2.2703(11), Ti(1)–Cl(2) 2.2655(11), Ti(1)–O(1) 1.771(2), Ti(2)–Cl(3) 2.3046(13), Ti(2)–O(2) 1.802(2), Ti(2)–O(3) 1.793(2), N(1)–C(1) 1.472(4), N(1)–C(18) 1.460(4), N(1)–C(27) 1.463(5) Å; Cl(1)–Ti(1)–Cl(2) 101.44(5), Cl(1)–Ti(1)–O(1) 101.03(8), Cl(2)–Ti(1)–O(1) 104.74(8), Cl(3)–Ti(2)–O(2) 100.36(10), Cl(3)–Ti(2)–O(3) 102.06(9), O(2)–Ti(2)–O(3) 106.52(10), Ti(1)–O(1)–C(3) 167.6(2), Ti(2)–O(2)–C(20) 170.0(3), Ti(2)–O(3)–C(29) 168.4(3), C(1)–N(1)–C(18) 111.8(2), C(1)–N(1)–C(27) 112.8(2), C(18)–N(1)–C(27) 110.6(3), N(1)–C(1)–C(2) 112.3(2), N(1)–C(18)–C(19) 114.1(3), N(1)–C(27)–C(28) 114.5(3)°.

titanium. The C(1)–N–C(20) bond angle [112.2(3)°] was rather larger than those in the others [C(1)–N–C(29), C(20)–N–C(29): 110.3(3), 110.0(3)°], whereas no significant differences were observed in N–C(1)–C(2), N–C(20)–C(21), and N–C(29)–C(30) bond angles [113.5(5), 113.8(3), 112.9(3)°, respectively].

Structure in the 1,2,4-$Me_3C_5H_2$ analogue (**3**) is similar to that in the Cp* analogue (**2**); the Ti(1)–Cl(1), Ti(1)–Cl(2), Ti(1)–O(1) bond distances [monophenoxide, 2.2703(11), 2.2655(11), 1.771(2) Å, respectively] are shorter than those in the bis(phenoxide) [Ti(2)–Cl(3), Ti(2)–O(2), Ti(2)–O(3): 2.3046(13), 1.802(2), 1.793(2) Å, respectively], whereas no significant differences in the Ti–O–C (in phenyl) bond angles were observed [Ti(1)–O(1)–C(3), Ti(2)–O(2)–C(20), Ti(2)–O(3)–C(29): 167.6(2), 170.3(3), 168.4(3)°, respectively]. The Ti–O–C bond angles in the Cp* analogue [**2**: 172.4(3)–174.0(3)°] were larger than those in the 1,2,4-$Me_3C_5H_2$ analogue [**3**: 167.6(2)–170.0(3)°].

As shown in Scheme 4, $[Cp^*TiMe_2\{(O\text{-}2,4\text{-}Me_2C_6H_2)\text{-}6\text{-}CH_2\}]_3N$ (**8**) could be prepared from Cp^*TiMe_3, prepared *in situ* by treating Cp^*TiCl_3 with MeLi in toluene, by reacting with $[(HO\text{-}2,4\text{-}Me_2C_6H_2)\text{-}6\text{-}CH_2]_3N$, although, as described above, attempted isolation of the dichloride analogue afforded the bimetallic complex, $[Cp^*TiCl_2\{(O\text{-}2,4\text{-}Me_2C_6H_2)\text{-}6\text{-}CH_2\}]$–$[Cp^*TiCl\{(O\text{-}2,4\text{-}Me_2C_6H_2)\text{-}6\text{-}CH_2\}_2]N$ (**2**). It was also revealed that the reaction of $[Cp^*TiCl_2\{(O\text{-}2,4\text{-}{}^tBu_2C_6H_2)\text{-}6\text{-}CH_2\}]_3N$ (**5**) with MeMgBr afforded the corresponding dimethyl complex (**9**), although the similar attempt for obtainment of **9** through one-pot synthesis from Cp^*TiCl_3 (at 25 °C overnight) failed and recovered both Cp^*TiMe_3 and $[(HO\text{-}2,4\text{-}{}^tBu_2C_6H_2)\text{-}6\text{-}CH_2]_3N$ (shown in the ESI†).[15] These complexes (**8** and **9**) were identified by NMR spectra and elemental analysis, and the structure of **9** could be determined by X-ray crystallographic analysis (shown in Fig. 4).

Complex **9** folds a distorted tetrahedral geometry around each titanium, and no significant differences in Ti–O, Ti–C (in methyl) bond distances, C(methyl)–Ti–C(methyl), Ti–O–C (in phenyl) angles *etc.* were observed in the three titanium complexes in **9**. The Ti–O bond distances in **9** [1.8149(17)–1.8230(17) Å] are longer than those in the dichloride analogue [**5**: 1.789(3)–1.792(3) Å], and Ti–O–C (in phenyl) bond angles in **9** [165.28(15)–166.02(16)°] are smaller than those in **5** [167.9(3)–169.8(3)°]. Moreover, the bond angles formed by two methyl group and titanium in **9** [95.20(13)–96.79(12)] are smaller than those formed by two chloride and the titanium in **5** [101.11(5)–101.85(6)].[17] These are observed trend between the dichloride and the dimethyl complex, exemplified by $Cp^*TiX_2(O\text{-}{}^iPr_2C_6H_3)$ [Ti–O, Ti–O–C (phenyl), X(1)–Ti–X(2): 1.772(3) Å, 173.0(3)°, 103.4(5)°, respectively (X = Cl); 1.790(2) Å, 168.7°, 99.8(1)°

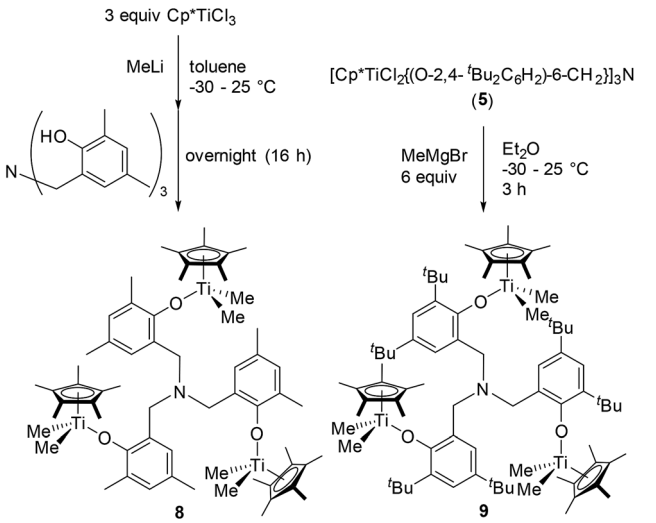

Scheme 4 Synthesis of $[Cp^*TiMe_2\{(O\text{-}2,4\text{-}R_2C_6H_2)\text{-}6\text{-}CH_2\}]_3N$ [R = Me (**8**), ^{t}Bu (**9**)].

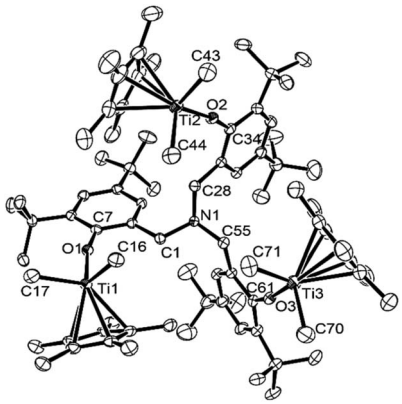

Fig. 4 ORTEP drawing for [Cp*TiMe$_2$\{(O-2,4-^{t}Bu$_2$C$_6$H$_2$)-6-CH$_2$\}]$_3$N (**9**). Thermal ellipsoids are drawn at the 50% probability level, and H atoms are omitted for clarity.[17] Selected bond distances (Å): Ti(1)–O(1) 1.8221(16), Ti(2)–O(2) 1.8230(17), Ti(3)–O(3) 1.8149(17), Ti(1)–C(16) 2.122(2), Ti(1)–C(17) 2.133(3), Ti(2)–C(43) 2.122(3), Ti(2)–C(44) 2.136(3), Ti(3)–C(70) 2.129(4), Ti(3)–C(71) 2.128(3), N(1)–C(1) 1.462(3), N(1)–C(28) 1.467(3), N(1)–C(55) 1.456(3). Selected bond angle (°): C(16)–Ti(1)–C(17) 95.63(10), C(43)–Ti(2)–C(44) 96.79(12), C(70)–Ti(3)–C(71) 95.20(13), Ti(1)–O(1)–C(7) 165.63(15), Ti(2)–O(2)–C(34) 165.28(15), Ti(3)–O(3)–C(61) 166.02(16).

(X = Me)],[14e] and rather small bond angles in **9**, described above, compared to those in **5** would be explained due to a steric bulk (rather large methyl group compared to Cl).

2. Ethylene polymerisation by [Cp′TiCl$_2$\{(O-2,4-R$_2$C$_6$H$_2$)-6-CH$_2$\}]$_3$N [R = Me, Cp′ = Cp (1); R = ^{t}Bu, Cp′ = Cp (4), Cp* (5), ^{t}BuC$_5$H$_4$ (6), 1,2,4-Me$_3$C$_5$H$_2$ (7)], [Cp′TiCl$_2$\{(O-2,4-Me$_2$C$_6$H$_2$)-6-CH$_2$\}][Cp′TiCl\{(O-2,4-Me$_2$C$_6$H$_2$)-6-CH$_2$\}$_2$]N [Cp′ = Cp* (2), 1,2,4-Me$_3$C$_5$H$_2$ (3)], and [Cp*TiMe$_2$\{(O-2,4-R$_2$C$_6$H$_2$)-6-CH$_2$\}]$_3$N [R = Me (8), ^{t}Bu (9)]

Table 2 summarises results in ethylene polymerisation at 25 °C in toluene using [Cp′TiCl$_2$\{(O-2,4-R$_2$C$_6$H$_2$)-6-CH$_2$\}]$_3$N [R = Me, Cp′ = Cp (**1**); R = ^{t}Bu, Cp′ = Cp (**4**), Cp* (**5**), ^{t}BuC$_5$H$_4$ (**6**), 1,2,4-Me$_3$C$_5$H$_2$ (**7**)], [Cp′TiCl$_2$\{(O-2,4-Me$_2$C$_6$H$_2$)-6-CH$_2$\}][Cp′TiCl\{(O-2,4-Me$_2$C$_6$H$_2$)-6-CH$_2$\}$_2$]N [Cp′ = Cp* (**2**), 1,2,4-Me$_3$C$_5$H$_2$ (**3**)], and [Cp*TiMe$_2$\{(O-2,4-R$_2$C$_6$H$_2$)-6-CH$_2$\}]$_3$N [R = Me (**8**), ^{t}Bu (**9**)] in the presence of methyl-aluminoxane (MAO) cocatalyst. MAO white solid, prepared by removing toluene and AlMe$_3$ from the commercially available sample [TMAO, 9.5 wt% (Al) toluene solution, Tosoh Finechem Co.], was employed because use of this MAO was effective in the ethylene (co)polymerisation for obtainment of (co)polymers with uniform molecular weight distributions.[10,14b,c,f]

It turned out that the Cp analogues (**1**, **4**) exhibited low catalytic activities affording ultrahigh molecular weight polymers with uniform molecular weight distributions (M_n = 2.02–3.58 × 10^6, M_w/M_n = 2.06–2.66, runs 1, 6–11 and runs S1 in Table S1 in the ESI†).[18] It also turned out that the activities at 25 °C by the 1,2,4-Me$_3$C$_5$H$_2$ analogues (**3** and **7**) and the ^{t}BuC$_5$H$_4$ analogue (**6**) were low and the resultant polymers prepared by **3** and **7** possessed bimodal molecular weight distributions (runs 5, 14, 15, runs S3, S6 and S7†), although slight improvement in the activity was observed by the bimetallic complex (**3**) compared to **1**. In contrast, it was revealed that the bimetallic Cp* analogue (**2**) and the Cp*-dimethyl analogues (**8**, **9**) exhibited higher catalytic activities (9060–16 800 kg PE per mol Ti per h, runs 2–4, 16–18) than the others, whereas the activity by the related Cp*-dichloride analogue (**5**) was low (384–428 kg PE per mol Ti per h, runs 12, S4†). The resultant polymers prepared by **8** and **9** possessed ultrahigh molecular weights with unimodal molecular weight distributions (M_n = 1.21–3.68 × 10^6, M_w/M_n = 2.16–3.16, runs 16–18, runs S9–S11 in the ESI†),[18] whereas the resultant polymers prepared by **2** possessed a mixture of ultrahigh and low molecular weights (runs 2–4, S2†) which might suggest a presence of two catalytically active species *in situ*. The observed polymerisation results are reproducible as shown in runs 6–11 as well as shown in the ESI.†[18]

It was revealed that the activities (on the basis of polymer yields) by [Cp′TiCl$_2$\{(O-2,4-^{t}Bu$_2$C$_6$H$_2$)-6-CH$_2$\}]$_3$N [Cp′ = Cp (**4**), Cp* (**5**), ^{t}BuC$_5$H$_4$ (**6**), 1,2,4-Me$_3$C$_5$H$_2$ (**7**)] increased at 50 °C, and the resultant polymers by both the Cp analogue (**4**) and ^{t}BuC$_5$H$_4$ analogue (**6**) possessed ultrahigh molecular weights with unimodal molecular weight distributions (M_n = 2.08–2.28 × 10^6, M_w/M_n = 2.04–2.48, runs 19, 20, S12, S13, Table 3 and ESI†).[18] Although notable improvement in the activity was observed when the polymerisation by **5** was conducted at 50 °C (run 24), the catalyst was short lived at 80 °C (runs 25, 26) and the activity decreased at 100 °C (run 27).[18] Moreover, the activity by **2** decreased upon increasing the polymerisation temperature (runs 22 and 23).[18] The dimethyl analogues (**8**, **9**) also showed the similar trends, and the activities decreased at 50 °C probably due to partial decomposition of the catalytically active species (runs 16, 17, 28–31, S21–S24†).[18]

Ethylene polymerisations using the mononuclear analogues, CpTiCl$_2$(O-2-R-4,6-Me$_2$C$_6$H$_2$) [R = Me (**10**), ^{t}Bu (**11**)], and Cp*TiCl$_2$(O-2-R-4,6-Me$_2$C$_6$H$_2$) [R = Me (**12**), ^{t}Bu (**13**)],[14b,c] were also conducted under the same conditions for comparison. Complexes **10** and **11** were prepared according the analogous procedure for synthesis of the Cp-aryloxo analogues (shown in the Experimental section).[10i,14b,c] The results are summarised in Table 4. The selected results by the trinuclear analogues, [Cp′TiCl$_2$\{(O-2,4-R$_2$C$_6$H$_2$)-6-CH$_2$\}]$_3$N [R = Me, Cp′ = Cp (**1**); R = ^{t}Bu, Cp′ = Cp (**4**), Cp* (**5**)] and [Cp*TiMe$_2$\{(O-2,4-R$_2$C$_6$H$_2$)-6-CH$_2$\}]$_3$N [R = Me (**8**), ^{t}Bu (**9**)], and bimetallic [Cp*TiCl$_2$\{(O-2,4-Me$_2$C$_6$H$_2$)-6-CH$_2$\}][Cp*TiCl\{(O-2,4-Me$_2$C$_6$H$_2$)-6-CH$_2$\}$_2$]N (**2**) are also placed for comparison.

It turned out that the activity by the Cp analogue, [CpTiCl$_2$\{(O-2,4-Me$_2$C$_6$H$_2$)-6-CH$_2$\}]$_3$N (**1**), was lower than that by CpTiCl$_2$(O-2,4,6-Me$_3$C$_6$H$_2$) (**10**) (runs 1, 32),[18] probably due to disproportionation of **1** (generating CpTiCl$_3$ exhibiting negligible activity)[14e] in the toluene solution as shown in Fig. 1. It also turned out that the activities by **4** were lower than those by the related mononuclear analogue (**11**) [runs 8, 19 (by **4**) *vs.* runs 33, 34 (by **11**)]. However, the resultant polymers prepared by **4** possessed unimodal molecular weight distributions suggesting a possibility that the polymerisation proceeded with uniform catalytically active species, whereas the resultant polymers prepared by **11** possessed the broad distributions (strongly

Table 2 Ethylene polymerisation by [Cp′TiCl$_2${(O-2,4-R$_2$C$_6$H$_2$)-6-CH$_2$}]$_3$N [R = Me, Cp′ = Cp (**1**); R = ^{t}Bu, Cp′ = Cp (**4**), Cp* (**5**), ^{t}BuC$_5$H$_4$ (**6**), 1,2,4-Me$_3$C$_5$H$_2$ (**7**)], [Cp′TiCl$_2${(O-2,4-Me$_2$C$_6$H$_2$)-6-CH$_2$}][Cp′TiCl{(O-2,4-Me$_2$C$_6$H$_2$)-6-CH$_2$}$_2$]N [Cp′ = Cp* (**2**), 1,2,4-Me$_3$C$_5$H$_2$ (**3**)], and [Cp*TiMe$_2${(O-2,4-R$_2$C$_6$H$_2$)-6-CH$_2$}]$_3$N [R = Me (**8**), ^{t}Bu (**9**)] in the presence of MAO cocatalyst (ethylene 4 atm, 25 °C)[a]

Run	Catalyst (μmol)	MAO/mmol	Time/min	Polymer/mg	Activity[b]	M_n[c] × 10^{-4}	M_w/M_n[c]
1	**1** (0.50)	3.0	10	80	320	341	2.13
2	**2** (0.03)	3.0	10	107	10 700	309, 3.91	2.11, 1.95
3	**2** (0.03)	3.0	5	78	15 600	368, 3.09	2.67, 2.19
4	**2** (0.03)	3.0	5	75	15 000	300, 1.93	2.29, 2.58
5	**3** (0.30)	3.0	10	116	1160	368, 0.96	1.72, 1.82
6	**4** (0.50)	2.0	10	120	480	220	2.13
7	**4** (0.50)	2.0	10	124	496	239	2.21
8	**4** (0.50)	3.0	10	186	744	204	2.44
9	**4** (0.50)	3.0	10	180	720	202	2.48
10	**4** (0.50)	4.0	10	140	560	238	2.64
11	**4** (0.50)	4.0	10	136	544	232	2.66
12	**5** (0.50)	3.0	10	107	428	172	2.90
13	**6** (0.50)	3.0	10	44	176	277	2.26
14	**7** (0.25)	3.0	10	75	600	93.1, 1.12	3.95, 2.11
15	**7** (0.25)	3.0	5	26	416	238, 0.97	2.75, 2.05
16	**8** (0.01)	3.0	10	84	16 800	214	2.20
17	**9** (0.10)	3.0	10	453	9060	354	2.24
18	**9** (0.01)	3.0	10	58	11 600	128	3.04

[a] Conditions: toluene total 30 mL, d-MAO (prepared by removing toluene and AlMe$_3$ from the ordinary MAO). [b] Activity in kg PE per mol Ti per h. [c] GPC data in *o*-dichlorobenzene *vs.* polystyrene standards.

Table 3 Effect of polymerisation temperature in ethylene polymerisation by [Cp*TiCl$_2${(O-2,4-Me$_2$C$_6$H$_2$)-6-CH$_2$}][Cp*TiCl{(O-2,4-Me$_2$C$_6$H$_2$)-6-CH$_2$}$_2$]N (**2**), [Cp′TiCl$_2${(O-2,4-^{t}Bu$_2$C$_6$H$_2$)-6-CH$_2$}]$_3$N [Cp′ = Cp (**4**), Cp* (**5**), ^{t}BuC$_5$H$_4$ (**6**), 1,2,4-Me$_3$C$_5$H$_2$ (**7**)], and [Cp*TiMe$_2${(O-2,4-R$_2$C$_6$H$_2$)-6-CH$_2$}]$_3$N [R = Me (**8**), ^{t}Bu (**9**)] in the presence of MAO cocatalyst[a]

Run	Catalyst (μmol)	Temp./°C	Time/min	Polymer/mg	Activity[b]	M_n[c] × 10^{-4}	M_w/M_n[c]
8	**4** (0.50)	25	10	186	744	204	2.44
19	**4** (0.10)	50	10	74	1480	215	2.04
13	**6** (0.50)	25	10	44	176	277	2.26
20	**6** (0.30)	50	10	58	387	226	2.48
14	**7** (0.25)	25	10	75	600	93.1, 1.12	3.95, 2.11
21	**7** (0.10)	50	10	43	860	220, 0.67	2.15, 1.62
2	**2** (0.03)	25	10	107	10 700	309, 3.91	2.11, 1.95
22	**2** (0.05)	50	10	140	8400	220, 1.44	1.67, 2.13
23	**2** (0.05)	80	10	65	3900	173, 0.95	1.47, 1.81
12	**5** (0.50)	25	10	107	428	172	2.90
24	**5** (0.10)	50	10	158	3160	113	2.85
25	**5** (0.10)	80	10	150	3000	26.4, 0.83	3.08, 1.63
26	**5** (0.10)	80	5	121	4840	37.7, 0.88	4.85, 1.64
27	**5** (0.10)	100	10	68	1360	112, 0.61	1.92, 1.68
16	**8** (0.01)	25	10	84	16 800	214	2.20
28	**8** (0.02)	50	10	128	12 800	215, 1.44	1.49, 2.06
29	**8** (0.02)	50	5	110	22 000	277, 2.09	2.33, 1.79
30	**8** (0.04)	80	10	84	4200	180, 0.96	1.53, 1.69
17	**9** (0.10)	25	10	453	9060	354	2.24
18	**9** (0.01)	25	10	58	11 600	128	3.04
31	**9** (0.05)	50	10	107	4280	126, 2.44	3.94, 1.53

[a] Conditions: toluene total 30 mL, d-MAO 3.0 mmol, ethylene 4 atm. [b] Activity in kg PE per mol Ti per h. [c] GPC data in *o*-dichlorobenzene *vs.* polystyrene standards.

suggesting a possibility that several catalytically active species were present *in situ*).

Note that the activities by the Cp* trinuclear analogue, [Cp*TiMe$_2${(O-2,4-Me$_2$C$_6$H$_2$)-6-CH$_2$}]$_3$N (**8**) showed higher catalytic activities than the related mononuclear analogue, Cp*TiCl$_2$(O-2,4,6-Me$_3$C$_6$H$_2$) (**12**) [runs 16, 28 (by **8**) *vs.* runs 35, 36 (by **12**)].[18] The activities by **2** and **8** were higher than those by Cp*TiCl$_2$(O-2-^{t}Bu-4,6-Me$_2$C$_6$H$_2$) (**13**) conducted under the same conditions (runs 2, 16, 28 *vs.* runs 37, 38). Although the activity by [Cp*TiCl$_2${(O-2,4-^{t}Bu$_2$C$_6$H$_2$)-6-CH$_2$}]$_3$N (**5**) at 25 °C was low, the activity increased at 50 °C (runs 12, 24), whereas no significant increase in the activity by **13** were observed at 50 °C (runs

Table 4 Summary of results in ethylene polymerisation by [Cp′TiCl$_2${(O-2,4-R$_2$C$_6$H$_2$)-6-CH$_2$}]$_3$N [R = Me, Cp′ = Cp (**1**); R = ^{t}Bu, Cp′ = Cp (**4**), Cp* (**5**)], [Cp*TiCl$_2${(O-2,4-Me$_2$C$_6$H$_2$)-6-CH$_2$}][Cp*TiCl{(O-2,4-Me$_2$C$_6$H$_2$)-6-CH$_2$}$_2$]N (**2**), and [Cp*TiMe$_2${(O-2,4-R$_2$C$_6$H$_2$)-6-CH$_2$}]$_3$N [R = Me (**8**), ^{t}Bu (**9**)], and Cp′TiCl$_2$(O-2-R-4,6-Me$_2$C$_6$H$_2$) [Cp′ = Cp, R = Me (**10**), ^{t}Bu (**11**); Cp′ = Cp*, R = Me (**12**), ^{t}Bu (**13**)] in the presence of MAO cocatalyst[a]

Run	Catalyst (μmol)	Cp′	R	Temp./°C	Polymer/mg	Activity[b]	M_n[c] × 10^{-4}	M_w/M_n[c]
1	**1** (0.50)	Cp	Me	25	80	320	341	2.13
32	**10** (0.50)	Cp	Me	25	110	1320	305	2.15
8	**4** (0.50)	Cp	^{t}Bu	25	186	744	204	2.44
19	**4** (0.10)	Cp	^{t}Bu	50	74	1480	215	2.04
33	**11** (0.50)	Cp	^{t}Bu	25	128	1540	30.3	7.69
34	**11** (0.50)	Cp	^{t}Bu	50	144	1730	78.4	4.35
2	**2** (0.03)	Cp*	Me	25	107	10 700	309, 3.91	2.11, 1.95
16	**8** (0.01)	Cp*	Me	25	84	16 800	214	2.20
28	**8** (0.02)	Cp*	Me	50	128	12 800	215, 1.44	1.49, 2.06
35	**12** (0.50)	Cp*	Me	25	430	5160	208	2.09
36	**12** (0.10)	Cp*	Me	25	173	10 400	139	2.71
12	**5** (0.50)	Cp*	^{t}Bu	25	107	428	172	2.90
24	**5** (0.10)	Cp*	^{t}Bu	50	158	3160	113	2.85
17	**9** (0.10)	Cp*	^{t}Bu	25	453	9060	354	2.24
18	**9** (0.01)	Cp*	^{t}Bu	25	58	11 600	128	3.04
31	**9** (0.05)	Cp*	^{t}Bu	50	107	4280	126, 2.44	3.94, 1.53
37	**13** (0.50)	Cp*	^{t}Bu	25	189	2270	26.0	9.33
38	**13** (0.50)	Cp*	^{t}Bu	50	199	2390	121	2.92

[a] Conditions: toluene total 30 mL, d-MAO 3.0 mmol, ethylene 4 atm, 10 min. [b] Activity in kg PE per mol Ti per h. [c] GPC data in *o*-dichlorobenzene *vs.* polystyrene standards.

Table 5 Ethylene polymerisation by [Cp*TiX$_2${(O-2,4-^{t}Bu$_2$C$_6$H$_2$)-6-CH$_2$}]$_3$N [X = Cl (**5**), Me (**9**)], [Cp*TiMe$_2${(O-2,4-Me$_2$C$_6$H$_2$)-6-CH$_2$}]$_3$N (**8**), Cp*TiCl$_2$(2-R-4,6-Me$_2$C$_6$H$_2$) [R = Me (**12**), ^{t}Bu (**13**)] in the presence of Al^{i}Bu$_3$/[Ph$_3$C][B(C$_6$F$_5$)$_4$] cocatalysts[a]

Run	Catalyst (μmol)	Al/Ti[b]	Temp./°C	Polymer/mg	Activity[c]	M_n[d] × 10^{-4}	M_w/M_n[d]
39	**5** (0.02)	700	25	71	7100	71.6	3.37
40	**8** (0.02)	100	25	Trace			
41	**8** (0.01)	300	25	60	12 000	71.6	3.78
42	**8** (0.01)	500	25	84	16 800	88.1	3.79
43	**8** (0.01)	700	25	138	27 600	115	3.15
44	**8** (0.01)	900	25	36	7200	70.8	3.33
45	**8** (0.01)	700	0	61	12 200	77.7	2.70
46	**8** (0.01)	700	0	70	14 000	78.4	2.70
47	**9** (0.02)	700	25	20	2000	78.5	4.21
48	**12** (0.03)	700	25	109	21 800	63.7	4.17
49	**13** (0.06)	700	25	85	8500	54.9	2.82

[a] Conditions: toluene total 30 mL, Al^{i}Bu$_3$, [Ph$_3$C][B(C$_6$F$_5$)$_4$] B/Ti = 1.5 (molar ratio), 4 atm, 10 min. [b] Molar ratio. [c] Activity in kg PE per mol Ti per h. [d] GPC data in *o*-dichlorobenzene *vs.* polystyrene standards.

37, 38).[18] Moreover, the activities by the dimethyl analogue, [Cp*TiMe$_2${(O-2,4-^{t}Bu$_2$C$_6$H$_2$)-6-CH$_2$}]$_3$N (**9**) were higher than those by **13** (runs 17, 31 *vs.* runs 37, 38) conducted under the same conditions. Therefore, we believe that these would be unique characteristics observed by placement of three titanium complexes in tris(phenoxy)amine ligand.

It was revealed that the activities in the ethylene polymerisation by [Cp*TiX$_2${(O-2,4-R$_2$C$_6$H$_2$)-6-CH$_2$}]$_3$N [R = ^{t}Bu, X = Cl (**5**); R = Me, X = Me (**8**), Table 5] in the presence of Al^{i}Bu$_3$–[Ph$_3$C][B(C$_6$F$_5$)$_4$] cocatalysts were higher than those in the presence of MAO under the optimized conditions (run 39 *vs.* run 12; run 43 *vs.* run 16).[18] Similar trends were observed in the mononuclear analogues (**12** and **13**), whereas the activity by **9** in the presence of Al^{i}Bu$_3$–[Ph$_3$C][B(C$_6$F$_5$)$_4$] cocatalysts was lower than that in the presence of MAO (run 47 *vs.* run 17). The trinuclear complex (**8**) exhibited the highest catalytic activities affording ultrahigh molecular weight polymer with uniform molecular weight distribution (27 600 kg PE per mol Ti per h, run 43, $M_n = 1.15 \times 10^6$, $M_w/M_n = 3.15$). The M_n values in addition to the activity by **8** was affected by the Al/Ti molar ratios (runs 40–44), and the polymerisations at 0 °C also afforded polymers with uniform molecular weight distributions without significant changes in the M_n values (runs 45, 46). These might suggest that the major chain transfer would not be the chain transfer to Al in this catalysis.

Concluding remarks

A series of trinuclear half-titanocenes, [Cp′TiCl$_2${(O-2,4-R$_2$C$_6$H$_2$)-6-CH$_2$}]$_3$N [R = Me, Cp′ = Cp (**1**); R = ^{t}Bu, Cp′ = Cp (**4**), Cp* (**5**),

^{t}BuC$_5$H$_4$ (**6**), 1,2,4-Me$_3$C$_5$H$_2$ (**7**)] and [Cp*TiMe$_2${(O-2,4-R$_2$C$_6$H$_2$)-6-CH$_2$}]$_3$N [R = Me (**8**), ^{t}Bu (**9**)], and the bimetallic complexes, [Cp′TiCl$_2${(O-2,4-Me$_2$C$_6$H$_2$)-6-CH$_2$}][Cp′TiCl{(O-2,4-Me$_2$C$_6$H$_2$)-6-CH$_2$}$_2$]N [Cp′ = Cp* (**2**), 1,2,4-Me$_3$C$_5$H$_2$ (**3**)], have been prepared and identified. Structures of **1–5**, **7** and **9** were determined by X-ray crystallography, and all complexes fold distorted tetrahedral geometries around titanium and Ti–O–C (phenyl) bond angles were affected by ligand substituents (on cyclopentadienyl, phenyl and halogen or methyl). It was revealed that these complexes (**2–9**) are stable in solution (25–80 °C) except the Cp analogue, [CpTiCl$_2${(O-2,4-Me$_2$C$_6$H$_2$)-6-CH$_2$}]$_3$N (**1**), that was unstable in solution and present as a mixture of the trinuclear complex (**1**), (proposed) binuclear analogue and CpTiCl$_3$ and titanatrane, CpTiCl[(O-2,4-Me$_2$C$_6$H$_2$)-6-CH$_2$]$_3$N; an equilibrium between **1** and the binuclear species (and CpTiCl$_3$) was observed depending upon temperature and concentration.

These complexes (**2–9**) exhibited from moderate to high catalytic activities for ethylene polymerisation in the presence of MAO cocatalyst, affording ultrahigh molecular weight polymers with uniform molecular weight distributions in most cases, especially in both the Cp and the Cp* analogues; different polymerisation behaviours compared to the related mononuclear analogues observed. In particular, the Cp* trinuclear analogue, [Cp*TiMe$_2${(O-2,4-Me$_2$C$_6$H$_2$)-6-CH$_2$}]$_3$N (**8**) showed higher catalytic activities than the related mononuclear analogue, Cp*TiCl$_2$(O-2-R-4,6-Me$_2$C$_6$H$_2$) [R = Me (**12**), ^{t}Bu (**13**)] conducted under the same conditions. The activities in the presence of Al^{i}Bu$_3$–[Ph$_3$C][B(C$_6$F$_5$)$_4$] cocatalysts were higher than those in the presence of MAO in most cases, although the M_n values in the resultant polymers decreased compared to those in the presence of MAO cocatalyst with rather broad molecular weight distributions. We thus believe that information observed here should be promising as an effect of integration of the catalytically active species, and would introduce a new possibility for design of efficient catalysts for olefin polymerisation.

Experimental section

1. General procedures

All experiments were carried out under a nitrogen atmosphere in a Vacuum Atmospheres drybox unless otherwise specified. All chemicals used were of reagent grade and were purified by the standard purification procedures. Anhydrous grades of toluene, *n*-hexane, and dichloromethane (Kanto Kagaku Co. Ltd) was transferred into a bottle containing molecular sieves (mixture of 3A and 4A 1/16, and 13X) in the drybox, and was used without further purification. Ethylene for polymerisation was of polymerisation grade (purity > 99.9%; Sumitomo Seika Co., Ltd.) and was used as received. Cp*TiCl$_2$(O-2-R-4,6-Me$_2$C$_6$H$_2$) [R = Me (**12**), ^{t}Bu (**13**)] were prepared according to the reported procedure.[14b,c] Toluene and AlMe$_3$ in the commercially available methylaluminoxane [TMAO, 9.5 wt% (Al) toluene solution, Tosoh Finechem Co.] were removed under reduced pressure (at *ca.* 50 °C for removing toluene, AlMe$_3$, and then heated at >100 °C for 1 h for completion) in the drybox to give white solids.[14c]

Elemental analyses were performed by using EAI CE-440 CHN/O/S Elemental Analyzer (Exeter Analytical, Inc.). All ^{1}H and ^{13}C NMR spectra were recorded on a Bruker AV500 spectrometer (500.13 MHz for ^{1}H, 125.77 MHz for ^{13}C). All spectra were obtained in the solvent indicated at 25 °C unless otherwise noted. Chemical shifts are given in ppm and are referenced to SiMe$_4$ (δ 0.00 ppm, ^{1}H, ^{13}C). Coupling constants are given in Hz. Molecular weights and molecular weight distributions for the resultant polymers were measured by gel permeation chromatography (Tosoh HLC-8121GPC/HT) using a RI-8022 detector (for high temperature; Tosoh Co.) with a polystyrene gel column (TSK gel GMHHR-H HT × 2, 30 cm × 7.8 mm i.d.), ranging from <10^2 to <2.8 × 10^8 MW at 140 °C using *o*-dichlorobenzene containing 0.05 w/v% 2,6-di-*tert*-butyl-*p*-cresol as the solvent. The molecular weight was calculated by a standard procedure based on the calibration with standard polystyrene samples.

Synthesis of [CpTiCl$_2${(O-2,4-Me$_2$C$_6$H$_2$)-6-CH$_2$}]$_3$N (1). Into diethyl ether (Et$_2$O) solution (20 mL) containing CpTiCl$_3$ (264 mg, 1.20 mmol) was added Et$_2$O solution (10 mL) containing [(LiO-2,4-Me$_2$C$_6$H$_2$)-6-CH$_2$]$_3$N (175 mg, 0.40 mmol), prepared by treating [(HO-2,4-Me$_2$C$_6$H$_2$)-6-CH$_2$]$_3$N with *n*-BuLi (equimolar to OH) in *n*-hexane at −30 °C and obtained as white precipitates, slowly at −30 °C. The stirred reaction mixture was then warmed slowly to room temperature, and the mixture was then stirred overnight (16 h). The solution was passed through a Celite pad, and the filter cake was washed with Et$_2$O. The combined filtrate and the wash were placed in a rotary evaporator to remove the volatiles. The resultant solid was dissolved in a minimum amount of CH$_2$Cl$_2$, and was then layered with *n*-hexane. The chilled solution placed in the freezer (−30 °C) afforded orange microcrystals (310 mg). Yield: 80%. ^{1}H NMR (500 MHz, toluene-d_8, −60 °C): δ 7.73 (s, 3H), 6.57 (s, 3H), 6.07 (s, 15H), 4.12 (bs, 6H), 2.40 (s, 9H), 2.21 (s, 9H). Anal. calcd C$_{42}$H$_{45}$Cl$_6$O$_3$NTi$_3$ (968.1): C, 52.11; H, 4.69; N, 1.45; found: C, 52.13; H, 4.97; N, 1.40.

Synthesis of [Cp*TiCl$_2${(O-2,4-Me$_2$C$_6$H$_2$)-6-CH$_2$}][Cp*TiCl{(O-2,4-Me$_2$C$_6$H$_2$)-6-CH$_2$}$_2$]N (2). The synthetic procedure for **2** was similar to that for **1**, except that Cp*TiCl$_3$ (234 mg, 0.80 mmol) in place of CpTiCl$_3$ (1.20 mmol) was used. The resultant solid after removal of Et$_2$O (and volatile) was dissolved in a minimum amount of CH$_2$Cl$_2$, and was then layered with *n*-hexane. The chilled solution placed in the freezer (−30 °C) afforded red microcrystals (123 mg). Yield: 35% (based on ligand). ^{1}H NMR (500 MHz, CDCl$_3$) δ 6.63 (s, 2H), 6.60 (s, 2H), 6.50 (s, 1H), 6.24 (s, 1H), 3.98 (d, J = 12.3 Hz, 2H), 3.47 (s, 2H), 3.34 (d, J = 12.3 Hz, 2H), 2.23 (s, 6H), 2.18 (s, 15H), 2.14 (s, 15H), 2.12 (s, 6H), 2.00 (s, 3H), 1.96 (s, 3H). ^{13}C NMR (126 MHz, CDCl$_3$) δ 161.7, 158.7, 132.6, 131.8, 131.1, 130.2, 129.6, 129.4, 128.6, 128.2, 127.9, 127.5, 126.9, 61.6, 51.2, 20.8, 20.6, 17.0, 16.9, 12.9, 12.4. Anal. calcd C$_{47}$H$_{60}$Cl$_3$O$_3$NTi$_2$ (889.1): C, 63.49; H, 6.80; N, 1.58; found: C, 63.74; H, 6.82; N, 1.47.

Synthesis of [(1,2,4-Me$_3$C$_5$H$_2$)TiCl$_2${(O-2,4-Me$_2$C$_6$H$_2$)-6-CH$_2$}][(1,2,4-Me$_3$C$_5$H$_2$)TiCl{(O-2,4-Me$_2$C$_6$H$_2$)-6-CH$_2$}$_2$]N (3). The synthetic procedure for **3** was similar to that for **1**, except that (1,2,4-Me$_3$C$_5$H$_2$)TiCl$_3$ (209 mg, 0.80 mmol) in place of CpTiCl$_3$ (1.20 mmol) was used. The resultant solid after removal of Et$_2$O (and volatile) was dissolved in a minimum amount of CH$_2$Cl$_2$,

and was then layered with *n*-hexane. The chilled solution placed in the freezer (−30 °C) afforded orange-red microcrystals (160 mg). Yield: 48% (based on ligand). ^{1}H NMR (500 MHz, $CDCl_3$) δ 6.73 (s, 1H), 6.68 (s, 2H), 6.65 (s, 2H), 6.40 (s, 1H), 6.15 (s, 2H), 6.10 (s, 2H), 4.05 (d, J = 12.9 Hz, 2H), 3.57 (s, 2H), 3.42 (d, J = 12.9 Hz, 2H), 2.23 (s, 6H), 2.18 (s, 6H), 2.17 (s, 12H), 2.15 (s, 3H), 2.12 (s, 3H), 2.09 (s, 3H), 2.03 (s, 3H). ^{13}C NMR (126 MHz, $CDCl_3$) δ 161.9, 161.3, 134.5, 134.4, 132.9, 131.1, 130.3, 130.2, 129.8, 129.4, 129.2, 128.4, 128.2, 127.4, 126.5, 121.3, 118.5, 60.6, 51.3, 20.9, 20.7, 17.0, 16.8, 16.2, 15.0, 14.6, 13.7. Anal. calcd $C_{47}H_{60}Cl_3O_3NTi_2$ (889.1): C, 62.00; H, 6.29; N, 1.68; found: C, 62.18; H, 6.40; N, 1.59.

Synthesis of [CpTiCl$_2${(O-2,4-^{t}Bu$_2$C$_6$H$_2$)-6-CH$_2$}]$_3$N (4). The synthetic procedure for **4** was similar to that for **1**, except that (LiO-2,4-^{t}Bu$_2$C$_6$H$_2$-6-CH$_2$)$_3$N (276 mg, 0.40 mmol) was used in place of (LiO-2,4-Me$_2$C$_6$H$_2$-6-CH$_2$)$_3$N. The resultant solid after removal of Et_2O (and volatile) was dissolved in a minimum amount of CH_2Cl_2, and was then layered with *n*-hexane. The chilled solution placed in the freezer (−30 °C) afforded red microcrystals (353 mg). Yield: 72%. ^{1}H NMR (500 MHz, $CDCl_3$) δ 7.70 (s, 3H), 7.20 (s, 3H), 6.67 (s, 15H), 3.95 (s, 6H), 1.38 (s, 27H), 1.21 (s, 27H). ^{13}C NMR (126 MHz, $CDCl_3$) δ 165.1, 146.6, 137.7, 130.9, 123.0, 122.1, 121.4, 55.1, 35.4, 34.8, 31.5, 30.6. Anal. calcd $C_{60}H_{81}Cl_6O_3NTi_3$ (1220.6): C, 59.04; H, 6.69; N, 1.15; found: C, 58.74; H, 6.90; N, 1.00.

Synthesis of [Cp*TiCl$_2${(O-2,4-^{t}Bu$_2$C$_6$H$_2$)-6-CH$_2$}]$_3$N (5). The synthetic procedure for **5** was similar to that for **4**, except that Cp*$TiCl_3$ (348 mg, 1.20 mmol) was used in place of $CpTiCl_3$. The resultant solid after removal of Et_2O (and volatile) was dissolved in a minimum amount of CH_2Cl_2, and was then layered with *n*-hexane. The chilled solution placed in the freezer (−30 °C) afforded red microcrystals (356 mg). Yield: 62%. ^{1}H NMR (500 MHz, $CDCl_3$) δ 8.09 (s, 3H), 7.21 (s, 3H), 4.11 (d, J = 16.8 Hz, 3H), 3.79 (d, J = 16.8 Hz, 3H), 1.98 (s, 45H), 1.36 (s, 27H), 1.26 (s, 27H). ^{13}C NMR (126 MHz, $CDCl_3$) δ 160.5, 145.2, 138.8, 133.27, 132.1, 121.7, 121.6, 52.7, 35.2, 34.8, 31.7, 30.7, 13.3. Anal. calcd $C_{75}H_{111}Cl_6O_3NTi_3$ (1431): C, 62.95; H, 7.81; N, 0.98; found: C, 62.86; H, 7.91; N, 0.97.

Synthesis of [(^{t}BuC$_5$H$_4$)TiCl$_2${(O-2,4-^{t}Bu$_2$C$_6$H$_2$)-6-CH$_2$}]$_3$N (6). The synthetic procedure for **6** was similar to that for **4**, except that (^{t}BuC$_5$H$_4$)$TiCl_3$ (331 mg, 1.20 mmol) was used in place of $CpTiCl_3$. The resultant solid after removal of Et_2O (and volatile) was dissolved in a minimum amount of CH_2Cl_2, and was then layered with *n*-hexane. The chilled solution placed in the freezer (−30 °C) afforded red microcrystals (324 mg). Yield: 56.2%. ^{1}H NMR (500 MHz, $CDCl_3$) δ 7.65 (d, J = 2.1 Hz, 3H), 7.19 (d, J = 2.3 Hz, 3H), 6.81 (t, J = 2.7 Hz, 6H), 6.11 (t, J = 2.7 Hz, 6H), 4.01 (s, 6H), 1.43 (s, 27H), 1.38 (s, 27H), 1.17 (s, 27H). ^{13}C NMR (126 MHz, $CDCl_3$) δ 165.2, 151.8, 146.3, 137.5, 130.8, 123.0, 122.0, 120.1, 119.6, 55.5, 35.4, 34.8, 34.1, 31.5, 30.9, 30.7. Anal. calcd for $C_{72}H_{105}Cl_6O_3NTi_3$ (1388.9): C, 62.54; H, 7.82; N, 0.99; found: C, 62.58; H, 7.63; N, 0.90.

Synthesis of [(1,2,4-Me$_3$C$_5$H$_2$)TiCl$_2${(O-2,4-^{t}Bu$_2$C$_6$H$_2$)-6-CH$_2$}]$_3$N (7). The synthetic procedure for **7** was similar to that for **4**, except that (1,2,4-Me$_3$C$_5$H$_2$)$TiCl_3$ (314 mg, 1.20 mmol) was used in place of $CpTiCl_3$. The resultant solid after removal of Et_2O (and volatile) was dissolved in a minimum amount of CH_2Cl_2, and was then layered with *n*-hexane. The chilled solution placed in the freezer (−30 °C) afforded red microcrystals (324 mg). Yield: 60%. ^{1}H NMR (500 MHz, $CDCl_3$) δ 7.97 (d, J = 2.1 Hz, 3H), 7.19 (d, J = 2.2 Hz, 3H), 5.99 (s, 6H), 4.03 (s, 6H), 2.16 (s, 18H), 1.98 (s, 9H), 1.36 (s, 27H), 1.24 (s, 27H). ^{13}C NMR (126 MHz, $CDCl_3$) δ 161.1, 145.7, 138.4, 135.0, 134.0, 131.7, 123.0, 122.1, 121.8, 54.1, 35.3, 34.8, 31.6, 30.3, 15.6, 14.5. Anal. calcd for $C_{69}H_{99}Cl_6O_3NTi_3$ (1346.9): C, 61.53; H, 7.41; N, 1.04; found: C, 61.66; H, 7.47; N, 0.97.

Synthesis of [Cp*TiMe$_2${(O-2,4-Me$_2$C$_6$H$_2$)-6-CH$_2$}]$_3$N (8). Into a toluene solution (18 mL) containing Cp*$TiCl_3$ (261 mg, 0.90 mmol) was added MeLi (2.75 mmol, in 2.5 mL Et_2O solution) slowly at −30 °C. The stirred reaction mixture was warmed slowly to room temperature, and the mixture covered by Al foil was then stirred for 3 h. Into the solution, toluene solution (6.0 mL) containing [(HO-2,4-Me$_2$C$_6$H$_2$)-6-CH$_2$]$_3$N (126 mg, 0.30 mmol) was then added by several portions at −30 °C, and the reaction mixture was warmed slowly to room temperature, and was then stirred overnight. The solution was then placed in a rotary evaporator to remove the volatiles. The residues were dissolved in *n*-hexane, and the solution was passed through a Celite pad, and the filter cake was washed with *n*-hexane. The combined filtrate and the wash were placed in a rotary evaporator to remove the volatiles. The crude product was dissolved in a minimum amount of *n*-hexane. The chilled solution placed in the freezer (−30 °C) afforded yellow microcrystals (262 mg). Yield 83%. ^{1}H NMR (500 MHz, $CDCl_3$) δ 7.44 (s, 3H), 6.79 (s, 3H), 3.64 (s, 6H), 2.26 (s, 9H), 2.10 (s, 9H), 1.81 (s, 45H), 0.42 (s, 18H). ^{13}C NMR (126 MHz, $CDCl_3$) δ 158.86 (s), 129.66 (s), 129.58 (s), 128.68 (s), 127.07 (s), 125.86 (s), 122.10 (s), 54.22 (s), 53.55 (s), 21.16 (s), 17.14 (s), 11.42 (s). Anal. calcd $C_{63}H_{93}O_3NTi_3$ (1056.0): C, 71.65; H, 8.88; N, 1.33; found: C, 71.49; H, 9.18; N, 1.27.

Synthesis of [Cp*TiMe$_2${(O-2,4-^{t}Bu$_2$C$_6$H$_2$)-6-CH$_2$}]$_3$N (9). Into an Et_2O solution (7.0 mL) containing [Cp*$TiCl_2${(O-2,4-^{t}Bu$_2$C$_6$H$_2$)-6-CH$_2$}]$_3$N (**5**) (71.6 mg, 0.05 mmol) was added MeMgBr (3 M in Et_2O, 0.10 mL) slowly at −30 °C. The stirred reaction mixture was warmed slowly to room temperature, and the mixture was then stirred for 3 h. The solution was placed in a rotary evaporator to remove the Et_2O. The resultant solid was dissolved in toluene and passed through a Celite pad, and the filter cake was washed with toluene. The combined filtrate and the wash were placed in a rotary evaporator to remove the volatiles. The resultant solid was dissolved in a minimum amount of toluene, and was then layered with *n*-hexane. The chilled solution placed in the freezer (−30 °C) afforded orange microcrystals (50 mg). Yield: 76.5%. ^{1}H NMR (500 MHz, $CDCl_3$) δ 7.98 (d, J = 2.1 Hz, 3H), 7.16 (d, J = 2.1 Hz, 3H), 3.39 (d, J = 3.5 Hz, 6H), 1.72 (s, 45H), 1.41 (s, 27H), 1.22 (s, 27H), 0.47 (s, 9H), 0.42 (s, 9H). ^{13}C NMR (126 MHz, $CDCl_3$) δ 159.52, 142.80, 137.06, 130.98, 122.87, 121.84, 121.29, 77.41, 77.16, 76.91, 58.35, 56.64, 53.92, 35.23, 34.71, 31.97, 30.76, 11.87. Anal. calcd $C_{81}H_{129}O_3NTi_3$ (1308.5): C, 74.35; H, 9.94; N, 1.07; found: C, 74.19; H, 9.76; N, 1.00.

Synthesis of CpTiCl$_2$(O-2,4,6-Me$_3$C$_6$H$_2$) (10). Complexes **10** was prepared according the analogous procedure for synthesis of the Cp-aryloxo analogues.[10i,14b,c] To an Et_2O solution (20 mL) containing $CpTiCl_3$ (219 mg, 1.00 mmol) was added LiO-2,4,6-

$Me_3C_6H_2$ (142 mg, 1.00 mmol) at −30 °C. The reaction mixture was warmed slowly to room temperature, and the mixture was then stirred overnight. The solution was passed through a Celite pad, and the filter cake was washed with Et_2O. The combined filtrate and the wash were placed in a rotary evaporator to remove the volatiles. The resultant solid was dissolved in a minimum amount of Et_2O, and was then layered with *n*-hexane. The chilled solution placed in the freezer (−30 °C) afforded brown microcrystals. Yield: 180 mg (56.4%). ^{1}H NMR (500 MHz, $CDCl_3$) δ 6.80 (s, 2H), 6.71 (s, 5H), 2.26 (s, 3H), 2.25 (s, 6H). ^{13}C NMR (126 MHz, $CDCl_3$) δ 165.4, 133.8, 129.0, 127.3, 120.8, 20.8, 17.2. Anal. calcd $C_{14}H_{16}Cl_2OTi$: C, 52.70; H, 5.06; found: C, 52.89; H, 4.97.

Synthesis of $CpTiCl_2$(O-2-^{t}Bu-4,6-$Me_2C_6H_2$) (11). The synthetic procedure for **11** was similar to that for **10**, except that LiO-2-^{t}Bu-4,6-$Me_2C_6H_2$ (184 mg, 1.0 mmol) was used in place of LiO-2,4,6-$Me_3C_6H_2$. Yield: 250 mg (69.2%). ^{1}H NMR (500 MHz, $CDCl_3$) δ 6.94 (s, 1H), 6.87 (s, 1H), 6.76 (s, 5H), 2.36 (s, 3H), 2.29 (s, 3H), 1.40 (s, 9H). ^{13}C NMR (126 MHz, $CDCl_3$) δ 165.8, 138.2, 133.4, 130.0, 129.4, 125.2, 121.1, 35.0, 30.4, 21.1, 18.9. Anal. calcd $C_{17}H_{22}Cl_2OTi$: C, 56.54; H, 6.14; found: C, 56.60; H, 6.11.

2. Polymerisation of ethylene

Reactions with ethylene were conducted in a 100 mL scale stainless steel autoclave, and the typical reaction procedure is as follows. Toluene (29.0 mL) and prescribed amount of MAO were added into the autoclave in the drybox. The reaction apparatus was then filled with ethylene (1 atm), and the prescribed amount of complex in toluene (1.0 mL) was added into the autoclave. The reaction apparatus was then immediately pressurized to 3 atm (total 4 atm), and the mixture was magnetically stirred for 5 or 10 min (ethylene pressure was kept constant during the reaction). After the above procedure, the mixture in the autoclave was poured into MeOH containing HCl, and the resultant polymer (white precipitate) was collected on a filter paper by filtration and was adequately washed with MeOH. The resultant polymer was then dried *in vacuo* at 60 °C for 2 h.

3. Crystallographic analysis

All measurements were made on a Rigaku XtaLAB P200 diffractometer using multi-layer mirror monochromated Mo-Kα radiation. The crystal collection parameters are listed in Tables S5 and S6 (ESI†). The data were collected and processed using CrystalClear (Rigaku)[19] or CrysAlisPro (Rigaku Oxford Diffraction),[20] and the structure was solved by direct methods[21] and expanded using Fourier techniques. The non-hydrogen atoms were refined anisotropically. Hydrogen atoms were refined using the riding model. All calculations were performed using the Crystal Structure[22] crystallographic software package except for refinement, which was performed using SHELXL Version 2014/7.[23] Details are shown in the ESI.†[17] CCDC numbers for complexes **1–5**, **7** and **9** are CCDC 1549581–1549587, respectively.

Conflicts of interest

There are no conflicts to declare.

Acknowledgements

This project was partly supported by Grant-in-Aid for Scientific Research (B) from the Japan Society for the Promotion of Science (JSPS, No. 15H03812). The authors express their thanks to Profs. S. Komiya, A. Inagaki, and Dr S. Sueki (Tokyo Metropolitan Univ.) for discussions, and to Tosoh Finechem Co. for donating MAO.

Notes and references

1 Selected reviews, accounts in 1990's, see: (*a*) R. F. Jordan, *Adv. Organomet. Chem.*, 1991, **32**, 325; (*b*) H. H. Brintzinger, D. Fischer, R. Mülhaupt, B. Rieger and R. M. Waymouth, *Angew. Chem., Int. Ed. Engl.*, 1995, **34**, 1143; (*c*) W. Kaminsky and M. Arndt, *Adv. Polym. Sci.*, 1997, **127**, 144; (*d*) J. Suhm, J. Heinemann, C. Wörner, P. Müller, F. Stricker, J. Kressler, J. Okuda and R. Mülhaupt, *Macromol. Symp.*, 1998, **129**, 1; (*e*) A. L. McKnight and R. M. Waymouth, *Chem. Rev.*, 1998, **98**, 2587; (*f*) G. J. P. Britovsek, V. C. Gibson and D. F. Wass, *Angew. Chem., Int. Ed.*, 1999, **38**, 428; (*g*) W. Kaminsky, *J. Chem. Soc., Dalton Trans.*, 1998, 1413.

2 Selected special issues: (*a*) Frontiers in Metal-Catalyzed Polymerization (special issue), J. A. Gladysz, *Chem. Rev.*, 2000, **100**, 1167; (*b*) Metallocene complexes as catalysts for olefin polymerization, H. G. Alt, *Coord. Chem. Rev.*, 2006, **250**, 1; (*c*) Metal-catalysed Polymerisation, B. Milani and C. Claver, *Dalton Trans.*, 2009, 8769; (*d*) Advances in Metal-Catalysed Polymerisation and Related Transformations, P. Mountford, *Dalton Trans.*, 2013, **42**, 8977.

3 Selected recent reviews/accounts, see: (*a*) The Lecture Notes in Chemistry 85, in *Organometallic Reactions and Polymerization*, ed. K. Osakada, Springer-Verlag, Berlin, 2014; (*b*) K. Nomura and S. Zhang, *Chem. Rev.*, 2011, **111**, 2342; (*c*) H. Makio, H. Terao, A. Iwashita and T. Fujita, *Chem. Rev.*, 2011, **111**, 2363; (*d*) M. Delferro and T. J. Marks, *Chem. Rev.*, 2011, **111**, 2450; (*e*) G. M. Miyake and E.-Y. X. Chen, *Polym. Chem.*, 2011, **2**, 2462; (*f*) C. Redshaw and Y. Tang, *Chem. Soc. Rev.*, 2012, **41**, 4484; (*g*) A. Valente, A. Mortreux, M. Visseaux and P. Zinck, *Chem. Rev.*, 2013, **113**, 3836; (*h*) J. P. McInnis, M. Delferro and T. J. Marks, *Acc. Chem. Res.*, 2014, **47**, 2545; (*i*) J. Klosin, P. P. Fontaine and R. Figueroa, *Acc. Chem. Res.*, 2015, **48**, 2004; (*j*) S. A. Ryken and L. L. Schafer, *Acc. Chem. Res.*, 2015, **48**, 2576; (*k*) B. L. Small, *Acc. Chem. Res.*, 2015, **48**, 2599.

4 (*a*) K. Nomura, J. Liu, S. Padmanabhan and B. Kitiyanan, *J. Mol. Catal. A: Chem.*, 2007, **267**, 1; (*b*) K. Nomura, *Dalton Trans.*, 2009, 8811; (*c*) K. Nomura and J. Liu, *Dalton Trans.*, 2011, **40**, 7666.

5 (*a*) D. W. Stephan, *Organometallics*, 2005, **24**, 2548; (*b*) M. J. Ferreira and A. M. Martins, *Coord. Chem. Rev.*, 2006, **250**, 118.

6 (*a*) *Coordination Polymerization*, ed. J. C. W. Chien, Academic Press, New York, 1975; (*b*) A. Andresen, H. G. Cordes, H. Herwig, W. Kaminsky, A. Merk, R. Mottweiler, J. Pein, H. Sinn and H. J. Vollmer, *Angew. Chem., Int. Ed. Engl.*, 1976, **15**, 630; (*c*) H. Sinn, W. Kaminsky, H.-J. Vollmer and R. Woldt, *Angew. Chem., Int. Ed. Engl.*, 1980, **19**, 390; (*d*) H. Sinn and W. Kaminsky, *Adv. Organomet. Chem.*, 1980, **18**, 99.

7 Selected review article, see: (*a*) A. Macchioni, *Chem. Rev.*, 2005, **105**, 2039; (*b*) M. Bochmann, *Organometallics*, 2010, **29**, 4711; (*c*) W. Kaminsky, *Macromolecules*, 2012, **4**, 3289; (*d*) S. Dagorne and C. Fliedel, in *Modern Organoaluminium Reagents, Topics in Organometallic Chemistry*, ed. S. Woodward and S. Dagorne, Springer-Verlag, Berlin-Heidelberg, 2013, vol. 41, p. 125.

8 (*a*) L. Li, M. V. Metz, H. Li, M.-C. Chen, T. J. Marks, L. Liable-Sands and A. L. Rheingold, *J. Am. Chem. Soc.*, 2002, **124**, 12725; (*b*) H. Li, L. Li, T. J. Marks, L. Liable-Sands and A. L. Rheingold, *J. Am. Chem. Soc.*, 2003, **125**, 10788; (*c*) N. Guo, L. Li and T. J. Marks, *J. Am. Chem. Soc.*, 2004, **126**, 6542; (*d*) H. Li, L. Li and T. J. Marks, *Angew. Chem., Int. Ed.*, 2004, **43**, 4937; (*e*) H. Li, L. Li, D. J. Schwartz, M. V. Metz, T. J. Marks, L. Liable-Sands and A. L. Rheingold, *J. Am. Chem. Soc.*, 2005, **127**, 14756; (*f*) H. Li and T. J. Marks, *Proc. Natl. Acad. Sci. U. S. A.*, 2006, **103**, 15295; (*g*) N. Guo, C. L. Stern and T. J. Marks, *J. Am. Chem. Soc.*, 2008, **130**, 2246; (*h*) A. Motta, I. L. Fragala and T. J. Marks, *J. Am. Chem. Soc.*, 2009, **131**, 3974.

9 (*a*) S. Liu, A. Motta, M. Delferro and T. J. Marks, *J. Am. Chem. Soc.*, 2013, **135**, 8830; (*b*) S. Liu, A. Motta, A. R. Mouat, M. Delferro and T. J. Marks, *J. Am. Chem. Soc.*, 2014, **136**, 10460.

10 For examples (by aryloxo-modified half-titanocene catalysts), see: (*a*) K. Nomura, H. Okumura, T. Komatsu and N. Naga, *Macromolecules*, 2002, **35**, 5388; (*b*) K. Nomura, M. Tsubota and M. Fujiki, *Macromolecules*, 2003, **36**, 3797; (*c*) W. Wang, M. Fujiki and K. Nomura, *J. Am. Chem. Soc.*, 2005, **127**, 4582; (*d*) K. Nomura, K. Itagaki and M. Fujiki, *Macromolecules*, 2005, **38**, 2053; (*e*) K. Nomura, K. Itagaki and M. Fujiki, *Macromolecules*, 2005, **38**, 8121; (*f*) F. Z. Khan, K. Kakinuki and K. Nomura, *Macromolecules*, 2009, **42**, 3767; (*g*) K. Kakinuki, M. Fujiki and K. Nomura, *Macromolecules*, 2009, **42**, 4585; (*h*) W. Apisuk and K. Nomura, *J. Polym. Sci., Part A: Polym. Chem.*, 2016, **54**, 1902; (*i*) W. Zhao, Q. Yan, K. Tsutsumi and K. Nomura, *Organometallics*, 2016, **35**, 1895.

11 (*a*) W. Wang, M. Fujiki and K. Nomura, *Macromol. Rapid Commun.*, 2004, **25**, 504; (*b*) P. M. Gurubasavaraj and K. Nomura, *Organometallics*, 2010, **29**, 3500; (*c*) Y. Takii, P. M. Gurubasavaraj, S. Katao and K. Nomura, *Organometallics*, 2012, **31**, 8237; (*d*) K. Nomura, U. Tewasekson and Y. Takii, *Organometallics*, 2015, **34**, 3272.

12 Synthesis of aryloxo-modified half-titanocenes supported on carbosilane dendrimers, see: (*a*) S. Arévalo, J. M. Benito, E. de Jesús, F. J. de la Mata, J. C. Flores and R. Gómez, *J. Organomet. Chem.*, 2000, **602**, 208; (*b*) S. Arévalo, E. de Jesús, F. J. de la Mata, J. C. Flores and R. Gómez, *Organometallics*, 2001, **20**, 2583; (*c*) S. Arévalo, E. de Jesús, F. J. de la Mata, J. C. Flores, R. Gómez, M. P. Gómez-Sal, P. Ortega and S. Vigo, *Organometallics*, 2003, **22**, 5109; (*d*) S. Arévalo, E. de Jesús, F. J. de la Mata, J. C. Flores, R. Gómez, M.-M. Rodrigo and S. Vigo, *J. Organomet. Chem.*, 2005, **690**, 4620. Ethylene polymerisation by half-titanocene supported on carbosilane dendrimer, $[[CpTiCl_2\{O\text{-}2,6\text{-}(MeO)_2C_6H_2\text{-}4\text{-}(CH_2)_3SiMe_2(CH_2)_3\}]_2SiMe(CH_2)_3]_4Si$ and $[CpTiCl_2\{O\text{-}2\text{-}MeC_6H_3\text{-}6\text{-}(CH_2)_2SiMe_2(CH_2)_3\}]_4Si$ in the presence of MAO cocatalyst. Latter complex showed the negligible activity.

13 Synthesis of the other trinuclear half-titanocenes, tris-1,3,5-$[Cp^*Ti(X_2)O]_3C_6H_3$ (X = Cl, Me). S. Arévalo, M. R. Bonillo, E. de Jesús, F. J. de la Mata, J. C. Flores, R. Gómez, P. Gómez-Sal and P. Ortega, *J. Organomet. Chem.*, 2003, **681**, 228.

14 Examples for synthesis, structural analysis of aryloxo-modified half-titanocenes (related to this study),[10i] see: (*a*) P. Gómez-Sal, A. Martín, M. Mena, P. Royo and R. Serrano, *J. Organomet. Chem.*, 1991, **419**, 77; (*b*) K. Nomura, N. Naga, M. Miki, K. Yanagi and A. Imai, *Organometallics*, 1998, **17**, 2152; (*c*) K. Nomura, N. Naga, M. Miki and K. Yanagi, *Macromolecules*, 1998, **31**, 7588; (*d*) S. J. Sturla and S. L. Buchwald, *Organometallics*, 2002, **21**, 739; (*e*) K. Nomura and A. Fudo, *Inorg. Chim. Acta*, 2003, **345**, 37; (*f*) K. Nomura, A. Tanaka and S. Katao, *J. Mol. Catal. A: Chem.*, 2006, **254**, 197.

15 Additional experiments for reactions of Cp^*TiCl_3 or $(1,2,4\text{-}Me_3C_5H_2)TiCl_3$ with $[(LiO\text{-}2,4\text{-}Me_2C_6H_2)\text{-}6\text{-}CH_2]_3N$, reaction of Cp^*TiMe_3 (generated *in situ*) with $[(HO\text{-}2,4\text{-}^tBu_2C_6H_2)\text{-}6\text{-}CH_2]_3N$, and additional VT ^1H NMR spectra for $[CpTiCl_2\{(O\text{-}2,4\text{-}Me_2C_6H_2)\text{-}6\text{-}CH_2\}]_3N$ (**1**) in toluene-d_8, and ^1H NMR spectra for $[Cp'TiCl_2\{(O\text{-}2,4\text{-}Me_2C_6H_2)\text{-}6\text{-}CH_2\}][Cp'TiCl\{(O\text{-}2,4\text{-}Me_2C_6H_2)\text{-}6\text{-}CH_2\}_2]N$ [Cp′ = Cp* (**2**), 1,2,4-$Me_3C_5H_2$ (**3**)], and $[Cp'TiCl_2\{(O\text{-}2,4\text{-}R_2C_6H_2)\text{-}6\text{-}CH_2\}]_3N$ [R = Me, Cp′ = Cp (**1**); R = ^{t}Bu, Cp′ = Cp (**4**), Cp* (**5**), ^{t}BuC$_5$H$_4$ (**6**), 1,2,4-$Me_3C_5H_2$ (**7**)] upon heating in toluene-d_8 at 80 °C (for 30 min) are shown in the ESI.†

16 L. Michalczyk, S. de Gala and J. W. Bruno, *Organometallics*, 2001, **20**, 5547.

17 Structural reports for $[CpTiCl_2\{(O\text{-}2,4\text{-}Me_2C_6H_2)\text{-}6\text{-}CH_2\}]_3N$ (**1**), $[Cp'TiCl_2\{(O\text{-}2,4\text{-}^tBu_2C_6H_2)\text{-}6\text{-}CH_2\}]_3N$ [Cp′ = Cp (**4**), Cp* (**5**), 1,2,4-$Me_3C_5H_2$ (**7**)], $[Cp'TiCl_2\{(O\text{-}2,4\text{-}Me_2C_6H_2)\text{-}6\text{-}CH_2\}][Cp'TiCl\{(O\text{-}2,4\text{-}Me_2C_6H_2)\text{-}6\text{-}CH_2\}_2]N$ [Cp′ = Cp* (**2**), 1,2,4-$Me_3C_5H_2$ (**3**)], and $[Cp^*TiMe_2\{(O\text{-}2,4\text{-}^tBu_2C_6H_2)\text{-}6\text{-}CH_2\}]_3N$ (**9**) are shown in the ESI.† CCDC numbers for complexes **1–5**, **7** and **9** are CCDC 1549581–1549587, respectively.†

18 Additional ethylene polymerisation results including confirmation of reproducibility are shown in the ESI.†

19 *CrystalClear: Data Collection and Processing Software*, Rigaku Corporation, Tokyo 196-8666, Japan, 1998–2015.

20 *CrysAlisPro: Data Collection and Processing Software*, Rigaku Corporation, Tokyo 196-8666, Japan, 1998–2015.

21 (*a*) G. M. Sheldrick, SHELXT, *Acta Crystallogr., Sect. A: Found. Adv.*, 2014, **70**, C1437; (*b*) A. Altomare, G. Cascarano, C. Giacovazzo and A. Guagliardi, SIR92, *J. Appl. Crystallogr.*, 1993, **26**, 343.

22 *Crystal Structure 4.2: Crystal Structure Analysis Package*, Rigaku Corporation, Tokyo 196-8666, Japan, 2000–2015.

23 G. M. Sheldrick, SHELXL Version 2014/7, *Acta Crystallogr., Sect. A: Found. Crystallogr.*, 2008, **A64**, 112.